Bulletin of Earthquake Engineering (2022) 20:5161–5203
https://doi.org/10.1007/s10518-022-01395-y

ORIGINAL ARTICLE

Vulnerability prediction model of typical structures considering empirical seismic damage observation data

Si-Qi Li[1,2,3] · **Hong-Bo Liu**[1,4]

Received: 18 January 2022 / Accepted: 26 March 2022 / Published online: 10 April 2022

Abstract

To deeply explore the seismic vulnerability characteristics of typical structures and obtain the differences in the seismic capacity of multiple structural categories in actual earthquakes, combined with mathematical statistics and probabilistic damage model analysis methods, the bulk of collection and statistics were made on the structural seismic damage observation data ($98{,}051.8122 \times 10^4$ m^2 and 995,269 buildings) of 213 destructive earthquakes in China from 1975 to 2013. Seismic damage sample databases of wooden roof truss structures, adobe and timber structures, brick wood structures, masonry structures, RC structures, and bottom frame seismic wall masonry structure were established. A seismic damage investigation and analysis were conducted. All samples' vulnerability grades were evaluated using the latest version of the Chinese seismic intensity scale (CSIS-20). The actual damage vulnerability probability matrix and surface model of structures in multiple intensity regions based on the investigated area and quantity parameters were established. A nonlinear regression prediction model analysis method was proposed. A typical structural vulnerability prediction model considering the failure ratio and exceedance probability in the multi-intensity region was established and verified by the earthquake damage database. In addition, a vulnerability matrix prediction model considering updating the mean vulnerability index parameter was proposed, and a comparison model of the vulnerability prediction matrix of typical regional structures was developed.

Keywords Typical building structure · Field observation data · Vulnerability prediction model · Vulnerability matrix · Update mean vulnerability index prediction model

✉ Si-Qi Li
lisiqi@hlju.edu.cn

✉ Hong-Bo Liu
hongboliuhlju@126.com

[1] School of Civil Engineering, Heilongjiang University, No. 74, Xuefu Road, Harbin City, China

[2] School of Transportation Science and Engineering, Harbin Institute of Technology, Harbin City, China

[3] Longjian Road and Bridge Co., Ltd, No. 109, Songshan Road, Harbin City, China

[4] Key Laboratory of Functional Inorganic Material Chemistry (Heilongjiang University), Ministry of Education, Harbin, Heilongjiang, People's Republic of China

1 Introduction

The occurrence of earthquakes is accidental and random. Earthquakes of different intensities significantly impact human production and life, especially damage to building structures, which directly or indirectly leads to casualties and property losses. The in-depth study of building structures' seismic vulnerability and capacity has become a hot topic in earthquake resistance engineering worldwide. Influenced by the factors of environment, economy, application, and regional culture, building structures show different structural forms in multiple historical periods, such as wooden roof truss structures (WRTSs), adobe and timber (AT) structures, brick wood (BW) structures, masonry structures (MSs), reinforced concrete (RC) structures and bottom frame seismic wall masonry (BFM) structures. These typical structures are widely used in developed and developing countries. According to the characteristics of their buildings, different regions worldwide have formulated typical structural seismic codes and macrointensity standards to improve their seismic capacity and postearthquake damage assessment. Many experts and scholars in the field of earthquake engineering and structural earthquake resistance have developed substantial research work from typical structural theory and numerical simulation analysis, reduced or full-scale model shaking table tests, and empirical structural vulnerability research based on actual earthquake damage.

Regarding the observational-based approaches of typical structures, researchers in different regions worldwide have conducted vulnerability analyses of various structural categories considering different parameter moduli. Ruggieri et al. (2020) conducted field seismic loss observations on 90 masonry churches in the Valley Scrivia Earthquake, Piemonte, Italy, in 2003 and used the ground peak acceleration (PGA) as an intensity measure to establish the vulnerability function model of MS based on this earthquake observation. Chen et al. (2017) conducted field observations on RC, MS, BW and AT, which were seriously damaged in the Mw 7.8 Gorkha earthquake in Nepal in 2015, analysed the seismic damage mechanism of various structures and proposed a technical path to improve the seismic capacity of the above structures. Dai et al. (2020) studied a field observation of the Lushan earthquake in China in 2013, established a finite element model combined with the actual damaged middle school gymnasium (composite structure of RC and steel frame), and performed a comparative analysis of the earthquake loss between the investigation background and numerical simulation. Avila-Haro et al. (2022) studied at the probabilistic nonlinear building model technology path of unreinforced masonry (URM) structures, combined with a typical observational structure in Barcelona, Spain, established a building model, analysed the correlation between material characteristics and damage parameters, and determined that the variability of masonry materials significantly affected the uncertainty of the seismic response of URM structures.

Combined with observational-based approaches, building damage characteristics, finite element models, functional models, machine learning research methods and rapid visual screening techniques were developed to study the vulnerability of typical structures (RC, MS, BFM). Chieffo et al. (2021), Kita et al. (2021), Briceño et al. (2021), Stocchi et al. (2021), Domaneschi et al. (2021) and Mulas et al. (2021) considered the influence of structural geometric characteristics, boundary conditions and cumulative damage modes, and the ground motion parameters detected by the virtual network were selected for nonlinear incremental dynamic and vulnerability model analysis. Clarke and Carey (2021) analysed mountain buildings in the dual Island Republic of Trinidad and Tobago. They established vulnerability function models (Zizi et al. 2021) of three types of mountain buildings by

using incremental dynamic and uncertainty analysis methods. Ruggieri et al. (2021) used the machine learning research method to build a new functional platform to evaluate the vulnerability of existing buildings, conducted vulnerability analysis by relying on photos of different building structure types, and verified the effect of this method with five buildings of different structure types. Shin et al. (2021) analysed the seismic damage mechanism of the weak floor of BFM, proposed an analysis method for rapid visual screening technology evaluation of structural damage using the seismic damage information modulus, and established a multidimensional curved surface damage model.

The empirical vulnerability analysis method can directly and effectively evaluate the damage characteristics and vulnerability of structures under different seismic intensities. Many structural seismic researchers investigate and analyse the structural damage after typical earthquakes and obtain distinct structural failure characteristics.

Taking a typical destructive earthquake as an example, a large number of structural seismic damage investigations were conducted. A multidimensional evaluation model for effectively measuring structural vulnerability was established using risk assessment methods, probability models, mathematical statistics, and vulnerability parameter analyses.

In terms of empirical vulnerability model analysis based on field observation data, Lovon et al. (2021) collected actual seismic damage data of more than 200 MSs in the earthquake region of Portugal. They constructed the damage model of average risk and structural seismic damage failure ratio (FR). Saretta et al. (2016), Gaudio et al. (2021), and Brando et al. (2021) conducted seismic damage investigations in the 2016 and 2009 in Italian, used macrointensity standards (EMS-98 and MCS) and probability model statistical methods to evaluate the vulnerability level and failure analysis of MS and BW, and established typical structural vulnerability models. Menichini et al. (2022) investigated the seismic damage of typical structures by using geographic information system (GIS) technology for the two destructive earthquakes in Lunigiana and Garfagnana, Italy, in 2013 (Grigoratos et al. 2021). The bulk of seismic damage statistics work was conducted, and constructed the empirical vulnerability curve of typical structures by using EMS-98 and peak ground acceleration (PGA). Biglari et al. (Biglari et al. 2021, 2022) investigated the seismic damage of historical buildings in specific earthquake regions in Iran, proposed a vulnerability assessment model considering 15 influencing factors, established the vulnerability probability curve of typical structures, and statistically provided the vulnerability probability matrix based on EMS-98. Bilgin et al. (2022) conducted a structural seismic damage investigation on the earthquake in Northwest Albania on November 26, 2019, analysed the actual seismic damage and failure mechanism of typical structures, took multistory MS as an example, conducted pushover response analysis, and obtained the structural vulnerability and failure modes under different PGAs.

In terms of empirical vulnerability analysis based on risk evaluation and statistical modelling, Altindal et al. (2021) used the probabilistic seismic risk assessment method to conduct empirical seismic damage prediction and assessment of typical structures in the remaining blocks in Istanbul, Turkey. They established the vulnerability probability model curves of RC and MS. Kechidi et al. (2021) proposed a risk model for evaluating structural seismic damage and conducted seismic damage risk and vulnerability analysis based on typical existing buildings in Algeria. Halder et al. (2021) collected six earthquake damage data in southeast India and Nepal in the past 10 years. They analysed and summarized the actual seismic damage characteristics of RC, MS, BW, and adobe structures by displaying typical earthquake damage survey pictures. Godínez-Domínguez et al. (2021) and Eudave et al. (2021) investigated and analysed the actual earthquake damage of structures and historical buildings in Mexico and

constructed multidimensional parameters for vulnerability assessment and acceleration time history analysis of typical structures. Combined with the seismic damage pictures of typical AT, BW, RC, and wooden frame buildings, the damage mechanism was analysed.

Qu et al. (2015) and Sun et al. (2021) conducted earthquake damage observations on the Lushan earthquake in China on April 20, 2013, focusing on the investigation and damage characteristics analysis of AT, BW, WRTS, and RC and established a vulnerability probability matrix according to the investigation sample data of typical earthquake regions. On May 12, 2008, a Mw 7.9 earthquake occurred in Wenchuan County, Sichuan Province, China, and a large number of buildings were seriously damaged. After the earthquake, the China Earthquake Administration organized experts and scholars worldwide to conduct an on-site inspection of structural earthquake damage, and a large number of inspection data of RC, MS, BFM, and BW (Li and Chen 2020; Li et al. 2019, 2021a) were collected. The empirical vulnerability database and damage matrix model of typical structures based on different intensity regions of the Wenchuan earthquake were established.

The above research uses different research methods to analyse the fragility and vulnerability of typical structures, which positively contributes to improving the seismic capacity of structures in various regions worldwide and the revision of building design codes. However, most studies mainly focus on the empirical vulnerability characteristics of a particular structural category under a specific earthquake. Theoretical and risk analysis has certain fuzziness and uncertainty in parameter setting, hazard model, and dynamic modulus, and the vulnerability parameter identification using PGA or PGV score has a certain singleness. By analysing the seismic damage of a single structure category in a specific earthquake, it is difficult to grasp the seismic vulnerability of various structures in the region as a whole.

This study collected and sorted the typical structural seismic damage observation data of 213 destructive earthquakes in 23 provinces (autonomous regions and municipalities directly under the central government) in China from 1975 to 2013. Combined with the on-site structural seismic damage observation characteristics, typical structures' failure mechanisms and characteristics were analysed. A large number of inspection data of WRTS, AT, BW, MS, RC, and BFM (China Earthquake Administration and National Bureau of Statistics 2001) (China Earthquake Administration and National Bureau of Statistics 1996) (China Earthquake Administration and National Bureau of Statistics 2005) were collected, and the empirical vulnerability database and damage matrix model of typical structures based on different intensity regions of the Wenchuan earthquake were established. The latest version of the China seismic intensity scale (CSIS-20) is employed to evaluate the vulnerability level of various structural seismic damage samples, and a typical structural vulnerability matrix model based on the investigated region and quantitative parameters was constructed. A nonlinear regression prediction model for evaluating and predicting the vulnerability of typical structures was proposed. The vulnerability comparison prediction model of typical structures considering multidimensional parameters in different intensity regions was established based on the sample database. The updated mean vulnerability index parameter model was proposed, and the regional vulnerability prediction model matrices of various typical structures were established. The seismic performance of various structures in different intensity regions was compared and analysed, which provides a necessary theoretical and practical reference for structural design and construction selection in other intensity regions and the revision of seismic design codes and intensity scales.

2 Actual seismic damage failure analysis of typical structures

Different levels of ground motion have caused varying degrees of earthquake damage to various structures. A great deal of historical earthquake damage observation data (China Earthquake Administration and National Bureau of Statistics 2001) (China Earthquake Administration and National Bureau of Statistics 1996) (China Earthquake Administration and National Bureau of Statistics 2005) indicates that the failure of engineering structures is an essential quantitative basis for casualties and property losses. According to the data statistics and relevant earthquake damage reports of 6 types of typical structures ($98{,}051.8122\times10^4$ m^2 and 995,269 buildings) investigated in 23 provinces (municipalities directly under the central government and autonomous regions) in China from 1975 to 2013, it was found that various structures suffer different levels of seismic damage in different periods and multiple intensity regions, especially in high-intensity regions, the damage was relatively heavy, and even the whole or local failure of the structure occurs. To grasp the vulnerability characteristics of typical structures relatively accurately, it was indispensable to analyse the failure mechanism of different structures.

2.1 Failure of WRTS

The primary structural system of WRTS is the wood frame. The roof adopts a slope structure, and wood purlins are arranged horizontally. This structure is extensively used in villages, towns, and mountainous areas in different world regions because of its suitable materials and relatively simple design and construction process. Most of these structures show good seismic performance in investigating historical earthquake damage because of their lightweight and relatively small seismic inertia force. According to the seismic damage observation data, the main damage characteristics were commonly the cracking damage of the filled wall and the seismic damage characteristics of the sliding tile on the roof. In high-intensity or extreme earthquake regions, some structures experience local or overall failures, as illustrated in Fig. 1.

The main reasons are excessive ground motion and long-term construction, failure to consider seismic design, poor construction technology, wood decay, and weathering, which are essential factors causing structural failure.

It shall be considered to conduct necessary reinforcement and anti-corrosion and anti-moth treatment of wooden materials for WRTS in the same or similar earthquake regions in combination with the actual on-site structural seismic damage characteristics and seismic design specifications to ensure that the structure meets the fortification intensity requirements and improve its overall lateral force capacity.

2.2 Failure of AT

AT is extensively used in developing countries because of its advantages of low construction cost, convenient material acquisition, simple structure, and low construction difficulty, especially in rural areas and areas with backwards economic development. Under the action of the earthquake, ATs in different regions were damaged to varying degrees. The adobe wall often cracks seriously or collapses, and the wood members are broken. Most of the AT in mountainous regions and villages did not consider seismic design; there are local failures or overall collapse of some structures in medium- and high-intensity regions, as depicted in Fig. 2. It should be regarded as conducting the necessary reinforcement

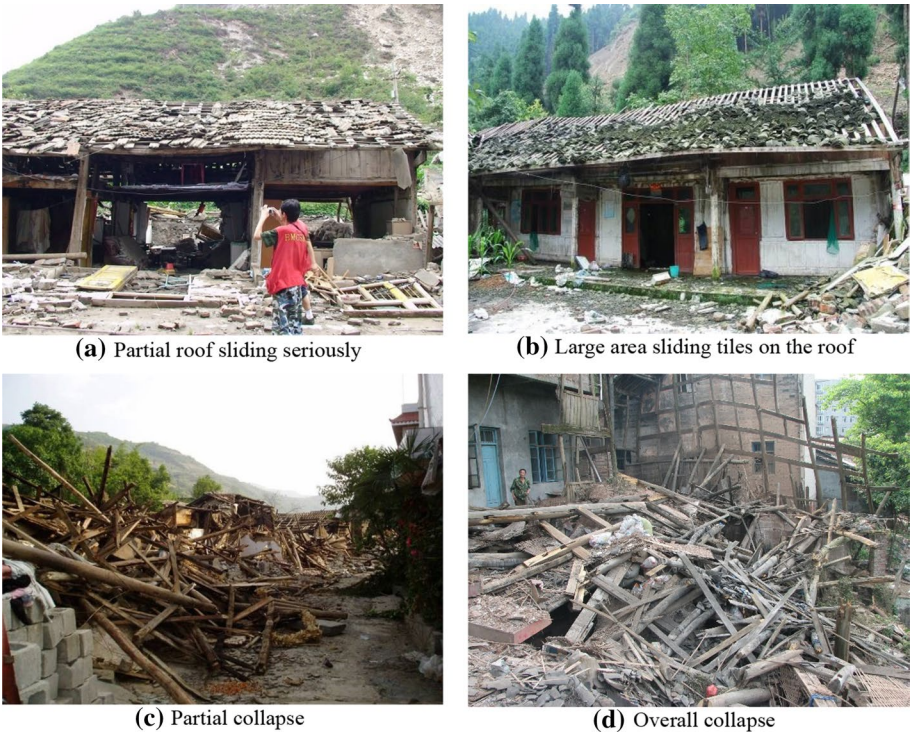

Fig. 1 Failure of WRTS

Fig. 2 Failure of adobe and timber structures

treatment for the old AT, increasing the connection between adobe and wood members, improving the overall structural stability, increasing anti-lateral force measures, improving the ability of the wall to resist horizontal ground motion, strictly standardizing the structural seismic design and construction, and ensuring that the AT structure has good strength, stiffness, and ductility.

2.3 Failure of BW

According to the observation data of historical earthquake-damaged structures, BW has a long construction history in different regions worldwide. Its primary stress system is brick masonry or wood components. The structural layout is relatively flexible, the brick and wood materials are convenient, and the price is low. It is widely used in villages and towns in many regions. This type of structure was subject to varying degrees of seismic damage under the action of an earthquake. The general seismic damage characteristics were brick masonry wall cracking, wood member failure due to weak connection, and roof failure. According to the actual seismic damage observation samples of BW (Li et al. 2021b), there was a seismic damage phenomenon of the local or overall collapse of some structures, as depicted in Fig. 3.

Considering the current earthquake damage observations in rural towns in different regions, with proper reference to the seismic code, high-quality brick masonry and wood

Fig. 3 Failure of BW structure (Li et al. 2021b)

are selected to strengthen BW to improve the overall stability and flexibility of BW structures. Due to the constraints of environmental and economic conditions, BW structures still have a massive stock in China and many developing countries. The improvement of the seismic performance of such structures should attract full attention in international construction, seismic, and design.

2.4 Failure of MS

MS has the advantages of relatively mature and straightforward construction technology, low material cost, good stress characteristics, and a short construction period. A large number of MSs have been built in different regions of the world. According to the seismic damage observation data of the Wenchuan and Yushu earthquake structures in China, the number of MSs was the largest. Most of these structures in different regions had relatively good seismic performance. However, there were still some damage characteristics of wall cracking or failure, oblique cracking at door and window openings, and structural column failure. In high-intensity regions, a small number of structures had a local or overall failure, as depicted in Fig. 4. Although this type of structural material was brittle, lacked flexibility, and had weak shear capacity, a large number of actual earthquake damage observation data (Li and Chen 2020; Li et al. 2021a) indicated that this type of structure showed good seismic performance, and its use should not be limited. It should be considered to improve the resistance capacity of the wall, reasonably set structural columns and ring beams, ensure

Fig. 4 Failure of MS

the reinforcement ratio of stirrups and bent reinforcement, and improve the overall stability and ductility of the structure.

2.5 Failure of RC

RC structures (frame buildings) have the characteristics of apparent stress, reasonable force transmission, flexible spatial layout, convenient material production and use, and mature design and construction technology. Therefore, this type of structure is widely used worldwide, and its seismic performance has always been a concern. According to the actual seismic damage investigation and the historical sample seismic damage data collected in this study, the RC structure has excellent seismic capacity, the seismic damage is relatively light in low- and medium-intensity areas, and some structures still do not collapse even in high-intensity and extreme earthquake areas.

However, a few RC structures still have seismic damage, mainly characterized by severe cracking or collapse of infilled walls, seismic damage of beam-column joints, and local or overall failure of individual structures, as reported in Fig. 5. According to the field inspection of seismic damage, the cracking or collapse of an infilled wall is a typical seismic damage feature of an RC frame structure. Nevertheless, this is precisely because the failure of the infilled wall absorbs a large amount of seismic energy, plays the role of energy dissipation and

(a) Overall failure of RC structure

(b) Partial collapse of RC under construction

(c) Integral failure of multiple story RC structure

(d) Overall failure of RC structure

Fig. 5 Failure of RC structure

damping, and protects or delays the development of seismic damage of the main structure to a certain extent, which has a particularly positive significance.

The column top, bottom, and beam-column joints are subjected to shear compression composite stress, resulting in plastic failure, concrete falling off, and reinforcement yield. The seismic damage of the column occurs before the beam. The contribution of an infilled wall to the overall seismic capacity of the structure should be considered, and it is suggested to be included in the seismic design code of RC structures. Exploring the design mechanism of the beam hinge and "strong column and weak beam" ensures that the building has excellent shear and compressive capacity and further improves the seismic ability of the RC structure.

2.6 Failure of BFM

A BFM is a composite structure with an RC frame structure on the bottom or two floors and a masonry structure on the upper floors. The type of structure has a large bay on the ground floor, which can be used for commercial purposes, and the superstructure can be used for residence or office. Therefore, it is widely used in different regions of the world. Due to the structure being a composite structure, it often has the stress characteristics of uncoordinated structural stiffness and deformation, resulting in serious seismic damage to the bottom floor or transition layer, overall failure of the second-floor slab, local collapse of the structure, and even serious seismic damage to the sitting floor (overall failure of the bottom floor or transition layer) under the action of strong ground motion, as depicted in Fig. 6. The design and construction shall be performed strictly according to the seismic design codes in different regions. The seismic wall should be reasonably set to improve the bottom floor stiffness appropriately, effectively control the interstory stiffness ratio, increase the overall ductility of the structure, improve the compressive and shear performance, and avoid structural failure caused by noncoordination of structural system stiffness and improper selection of construction methods and materials.

2.7 Summary

According to the study of the actual structural damage samples of 213 destructive earthquakes in the Chinese mainland from 1975 to 2013, the abovementioned six typical structures have various destructive characteristics in different regions. A large number of houses designed and constructed according to the structural seismic design code have shown excellent seismic performance, and the seismic fortification goal of "not bad in the small earthquake, repairable in a medium earthquake and not falling in a large earthquake" has been realized. It should be considered that the matching seismic fortification and structural measures should be reasonably set according to the typical structural categories and actual seismic damage characteristics to achieve the goal of improving the seismic performance of various structures.

3 Observation and analysis of actual seismic damage of typical structures

To effectively evaluate and predict the actual seismic vulnerability characteristics of typical structures and deeply compare the seismic capacity of 6 types of structures under different intensity levels, the structural seismic damage observation data (China Earthquake

(a) Bottom failure of BFM structure

(b) Transition layer failure of BFM structure

(c) Failure of second-floor slab

(d) Local collapse of BFM structure

Fig. 6 Failure of BFM structure

Administration and National Bureau of Statistics 2001) (China Earthquake Administration and National Bureau of Statistics 1996) of 213 destructive earthquakes in 23 provinces (autonomous regions and municipalities directly under the central government) in China from 1975 to 2013 were collected and summarized. The database of structural seismic damage investigation samples (area and quantity) of WRTS, AT, BW, MS, RC, and BFM was established (see Supplementary data 1). The distribution zoning map of actual investigation samples was established, as depicted in Fig. 7. After the bulk of statistics and calculation of sample data, each province's regional survey sample parameters (area and quantity) were obtained, as summarized in Table 1 (due to the unitary characteristics of the structural category in a few earthquake regions and the influence of many uncertain factors on the investigation environment, the observation could only be carried out according to the area or number of buildings; for instance, in the earthquake region investigated in SD Province, there are only AT buildings investigated according to the number parameter, and all samples of BFM are observed according to the number). According to the actual seismic damage observation data of 6 types of typical structures, many classified statistics were performed according to different provinces (autonomous regions and municipalities directly under the central government), seismic frequencies, investigated building areas, quantities, and ages, as provided in Fig. 8.

According to the statistical results of the actual seismic damage survey sample data of typical structures, the frequency of destructive earthquakes in YN, XJ, SC, and QH

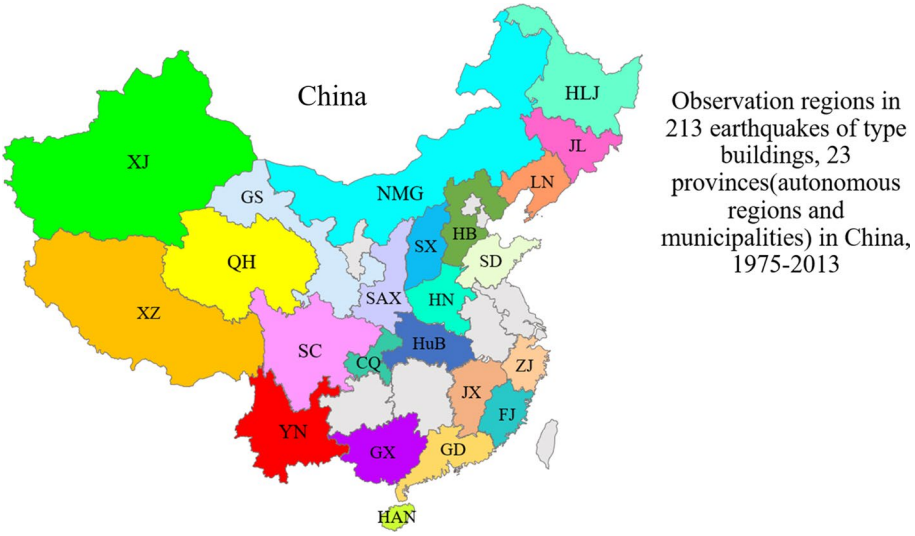

Fig. 7 Regional distribution of structural seismic damage investigation samples

provinces is relatively high, and the actual on-site seismic damage survey times of RC, MS, BW, and AT structures are greater than those of other structural categories. In the overall sample survey region, the survey area of earthquake damage is significantly higher than that of other structural categories. WRTS, BW, and MS are relatively balanced, and the survey area of the RC structure is relatively small.

In terms of the number of investigations, AT and BW are significantly greater than other structural categories, indicating to a certain extent that the stock of these two types of structures is enormous, and various degrees of earthquake damage have occurred in different periods and regions. In 2003 and 2008, the earthquake frequency causing damage to typical structures was relatively high, and the investigation frequency of MS, BW, and AT in different years was relatively high. Regarding the survey area and quantity in different regions, YN has the largest survey area of AT structure, and a large number of survey samples are concentrated in 1996, 2001, 2003, and 2008, with relatively more SC and XJ. HB and QH were focused in 1976 and 2010 due to many MS and AT. According to the regional distribution, age, seismic damage frequency, and stock characteristics of the above six types of typical structures, the structural seismic design measures and construction methods should be further modified to improve the seismic performance of various typical structures.

4 Comparison of empirical vulnerability prediction models of typical structures

Seismic vulnerability is an essential part of disaster risk analysis. Evaluating building structure vulnerability is of fundamental and guiding significance for postearthquake loss statistics and seismic design. The field empirical structural vulnerability study considers real earthquake damage as the background. It relies on vast amounts of actual structural seismic damage investigation data, effectively evaluating and predicting the structural

Table 1 Sample statistics of seismic damage observations of typical structures in China from 1975 to 2013

Survey region	Structure type Observation parameter (Area (A) 10^4m^2, Number (*N*))										
	WRTS	WRTS	AT	AT	BW	BW	MS	MS	RC	RC	BFM
	A	N	A	N	A	N	A	N	A	N	N
CQ			1177.075		24.3332		1340.544		23.5247		
FJ			97.2347		45.7105		90.3426		7.1		
GS			1436.25	2581	437.2827		1598.2738		6.5731		
HAN			3.6679								
HB			1160.541	61,486	338.1919		574.5648	409,346			
HLJ			63.4723		19.42		5.65				
HuB			37.55	2666	2.6	161	18.6465	1714			
JX			2385.24		64.3352		928.6716		1306.727		
JL			120.5375		35.3594						
LN				34,136			1709	18,366			
NMG			739.4891		862.988		101.4095				
QH	1.978		418.3366	316,433	306.049		597.6337		157.9257		
SD				869							
SX			59.9	32,077	19.5715	46,026	9.7560	145		51	70
SC	4334.6		5348.96	2488	1986.164	2269	1587.0494	16,623	253.3707	5712	5580
XJ	9.52		4795.92	14,436	2491.677		2420.5206		555.7603		
XZ			321.3987		214.6236		107.0115		75.0118		268
YN	7997.3	21,490	35,947.27	5	4604.153		4659.1255	236	1736.535	81	371
ZJ			0.1543				0.1543				
SAX			81.5005								
GD					22.9		104.3				
GX					18.0436		18.335				
HN					27						

Table 1 (continued)

Survey region	Structure type Observation parameter (Area (A) $10^4 m^2$, Number (*N*))										
	WRTS	WRTS	AT	AT	BW	BW	MS	MS	RC	RC	BFM
	A	N	A	N	A	N	A	N	A	N	N
Total	12,343.4	21,490	54,194.49	467,177	11,520.4	48,456	15,870.9888	446,430	4122.528	5844	6289

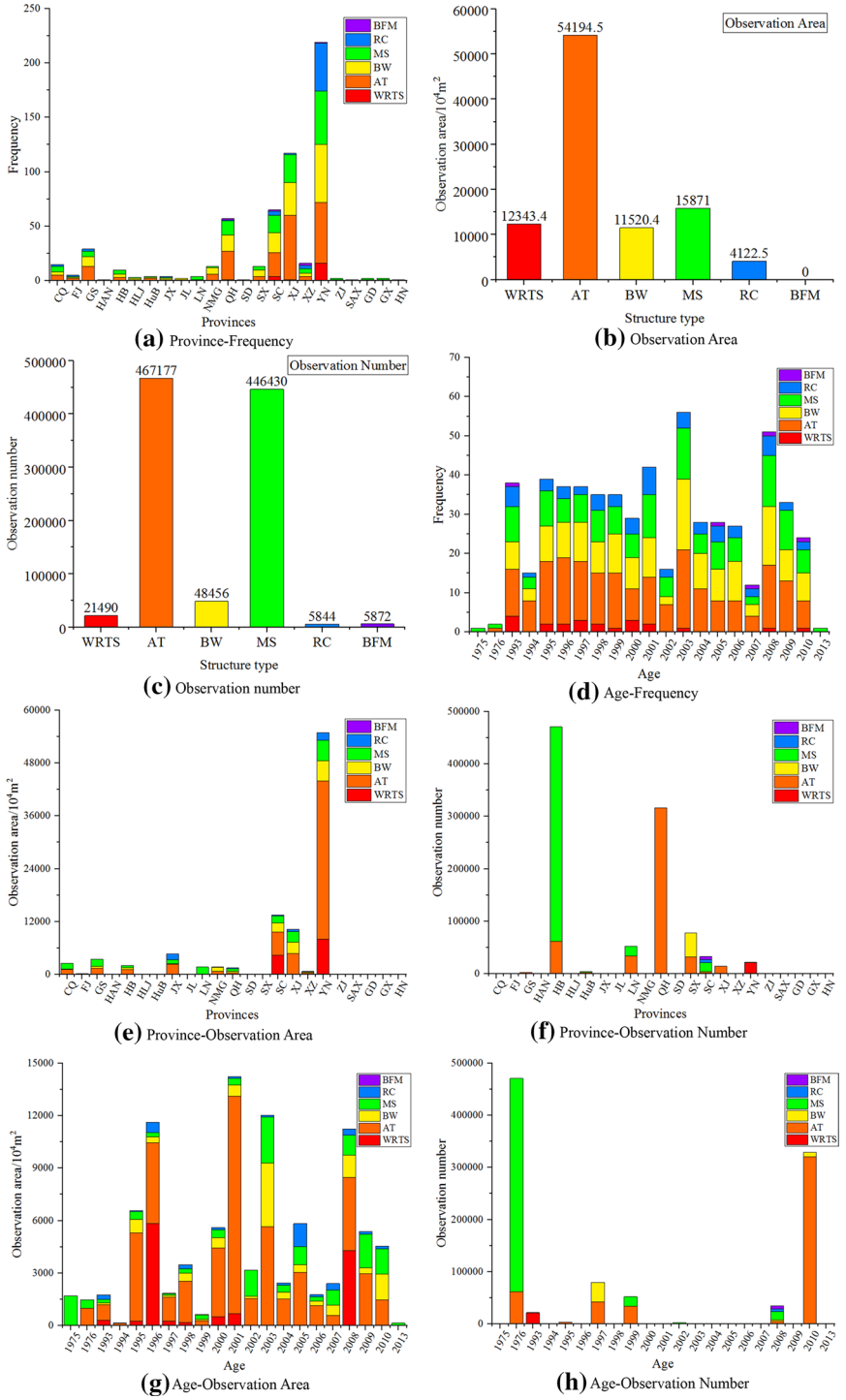

Fig. 8 Statistics of damage characteristics of typical structures under multidimensional parameter evaluation

seismic damage. According to the investigation of structural seismic damage in many earthquake sites, it is found that different structural seismic damage response parameters (investigation area and quantity) have a significant impact on its vulnerability. To deeply study the vulnerability characteristics of various typical structures under the influence of the above factors and analyse the differences in the vulnerability of typical structures under the influence of multiple parameters, vulnerability prediction and evaluation model comparative analysis should be conducted on six types of typical structures from multiple dimensional parameters.

4.1 Typical structural vulnerability surface model

Combining the assessment methods of mathematical statistics, numerical analysis, and risk prediction models, the vulnerability grades of $98{,}051.8122 \times 10^4$ m^2 and 995,269 buildings in all structural seismic damage sample databases are evaluated by using the vulnerability grade (VG) delimitation criteria (Basically intact, Slightly damaged, Moderately damaged, Severely damaged, and Destruction (DS1–DS5, (1, 2, 3, 4 and 5)) of the latest version of the China seismic intensity scale (CSIS-20). According to the quantification of the actual seismic damage failure ratio (FR) parameter of the structure, the actual damage vulnerability probability matrix (VPM) of WRTS, AT, BW, MS, RC, and BFM are established (see supplementary data 2), and the number distribution of typical structural vulnerability matrices (1342 in total) is statistically obtained, as indicated by Table 2.

To effectively analyse the actual seismic vulnerability of WRTS, AT, BW, MS, RC, and BFM in 23 provinces in China, the bulk of statistics and vulnerability analysis is performed on the overall sample database of structural seismic damage in different intensity regions. Using the damage probability analysis method, statistical theory, and three-dimensional model calculation and application technology, after a great deal of programming and mathematics, we found that the failure ratio (FR), VPM and vulnerability level/grade (VG) have a certain correlation. To more clearly compare the empirical vulnerability characteristics of six types of structures under the new dimension (surface model), the VPMs of various structures are sorted, and a multiple parameter vulnerability surface model based on the investigated area and quantity is constructed by using the three-dimensional model numerical method, as illustrated in Figs. 9, 10, 11, 12 and 13 (number of VPM axis indicates the sequence code of VPM).

Table 2 Quantity distribution of the structural seismic vulnerability matrix

Intensity	Number of typical structural vulnerability matrices											
	WRTS		AT		BW		MS		RC		BFM	
	A	N	A	N	A	N	A	N	A	N	A	N
VI	25	1	203	21	140	14	144	20	60	11		8
VII	17		109	24	57	14	50	23	21	23		14
VIII	9		37	21	26	14	23	29	8	20		15
IX	6		6	22	4	14	7	22	4	12		15
X			1	5		2		5		2		3
XI				5				3		1		2
Total	57	1	356	98	227	58	224	102	93	69	0	57

The vulnerability surface models of six typical structures based on 1342 vulnerability matrices analyse the damage characteristics of various structures in different intensity regions through three-dimensional models. They intuitively express the relationship between failure characteristics, vulnerability level, and probability matric clusters of various structures in multiple intensity regions.

According to the analysis results of the vulnerability matrix and surface model of various typical structures, in terms of survey area parameters, in the degree region of VI, the number of AT vulnerability matrices is the largest, the seismic damage is relatively heavy, the overall seismic damage survey samples and matrices of BW are large, the seismic damage of WRTs and MS are similar, and the seismic damage of RC and BFM is relatively light. In the degree region of VII, there are many AT, BW, and MS vulnerability matrices, and the damage degree of AT and BW is relatively severe, but there are still some samples at the DS1 and DS2 levels.

The number of sample vulnerability matrices in the degree region of VIII is relatively uniform, and most structures have severe seismic damage. A certain proportion of survey samples of WRTS, BW, and MS have damage of DS3 or above, but RC structures still have a certain number of seismic damage matrices at DS1 and DS2 levels. In the degree IX–XI regions, the number of vulnerability matrices of the investigated area parameter is relatively small, the seismic damage of the AT structure is relatively heavy, and even most of the overall structure failure occurs. The MS damage is slightly lighter than that of the BW structure.

In terms of the investigation quantity parameters, in the degree region of VI, the number of WRTS samples is small, and the seismic damage is relatively heavy. The numbers of AT and MS matrices are similar. Nevertheless, the overall damage of the former is heavier than that of the latter, the deterioration of BFM and MS is similar, and the damage of RC samples is light. The number of AT vulnerability sample matrices in the degree region of VII is the largest. Nevertheless, the overall seismic injury is relatively severe, and the number and seismic damage of the BW and MS matrices are similar. In the degree region of VIII, there are many MS matrices, the injury of AT samples is relatively serious, and the damage of some MS samples is slightly heavier than BFM. In the degree regions of IX–XI, all structures have severe earthquake damage. Some matrices indicate that AT and BW structures have a large proportion of DS4 and DS5 damage in the high-intensity region. However, there are still many vulnerability matrices for MS and RC structures, even in the degree region of XI.

According to the vulnerability statistics and analysis of the above six typical structures, the AT structure has relatively heavy seismic damage in different intensity regions. The reason is that this type of structure generally has not undergone seismic design. Most of them are houses self-built by rural and mountainous residents. Most of them are affected by economic conditions and are not constructed following the design specifications. The survey area and the number of BW samples are relatively large, and the damage is relatively serious in the medium–high intensity region. This type of structure is composed of masonry and wood frames. The mechanical characteristics are relatively complex, and the connection between structural members is relatively weak, resulting in insufficient structural integrity. The WRTS vulnerability matrix is relatively small, and is mainly established based on the investigated area parameter. The damage is relatively small in the medium- and low-intensity regions. Most of the damage characteristics are reflected in the falling of roof tiles and the cracking of maintenance structures. The RC structure exhibits excellent seismic performance in the overall vulnerability surface model analysis. Even in the extreme earthquake area, there are still

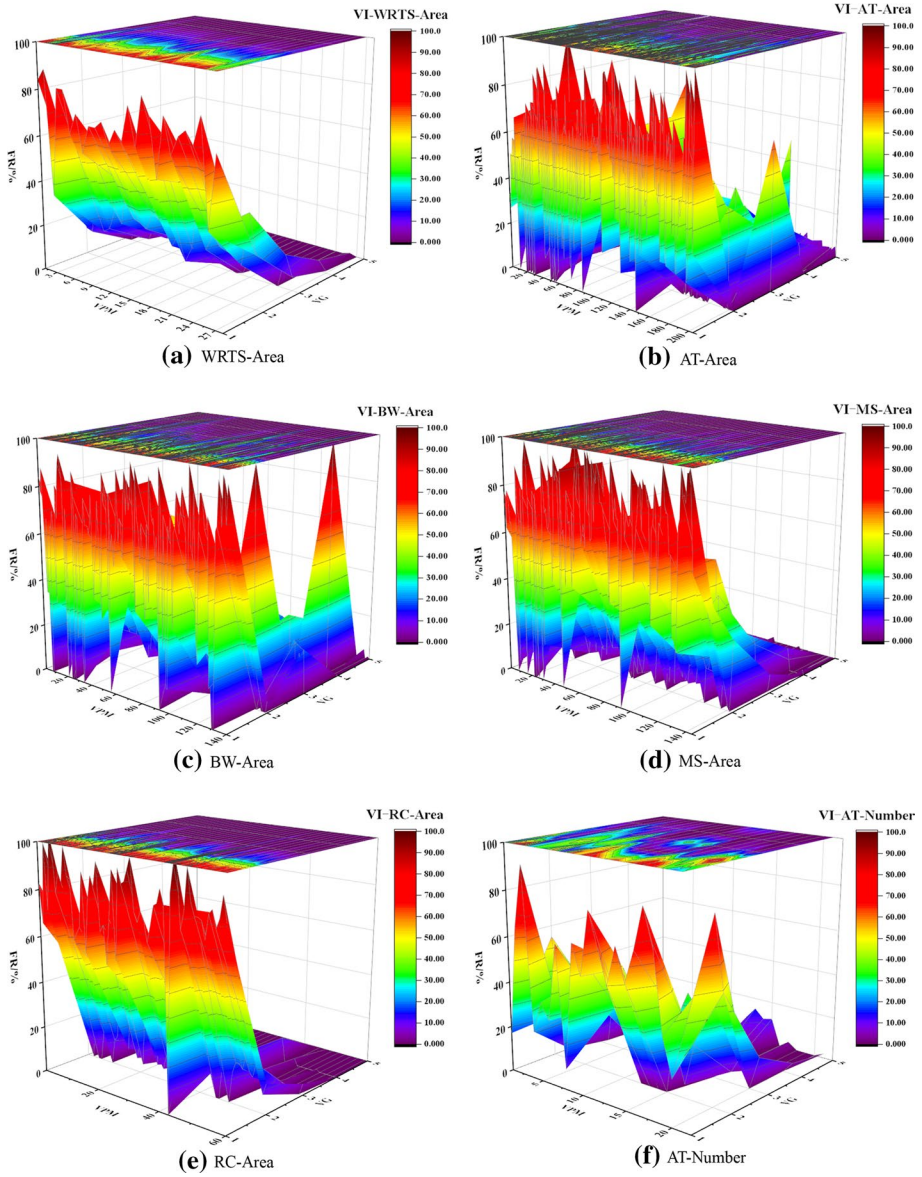

Fig. 9 Vulnerability surface model of the typical structure in degree region of VI

a certain number of matrices and samples, and the vulnerability of FR is at the lower vulnerability level.

Although the material of MS is brittle, the vulnerability surface model shows that its overall seismic performance is also relatively good, especially in the middle- and low-intensity areas. There are many samples, and the seismic damage is relatively light. BFM is an RC and MS composite structure system. The damage situation is similar to the two types of structures. The difference is slight in the medium- and low-intensity areas, but the seismic damage of this

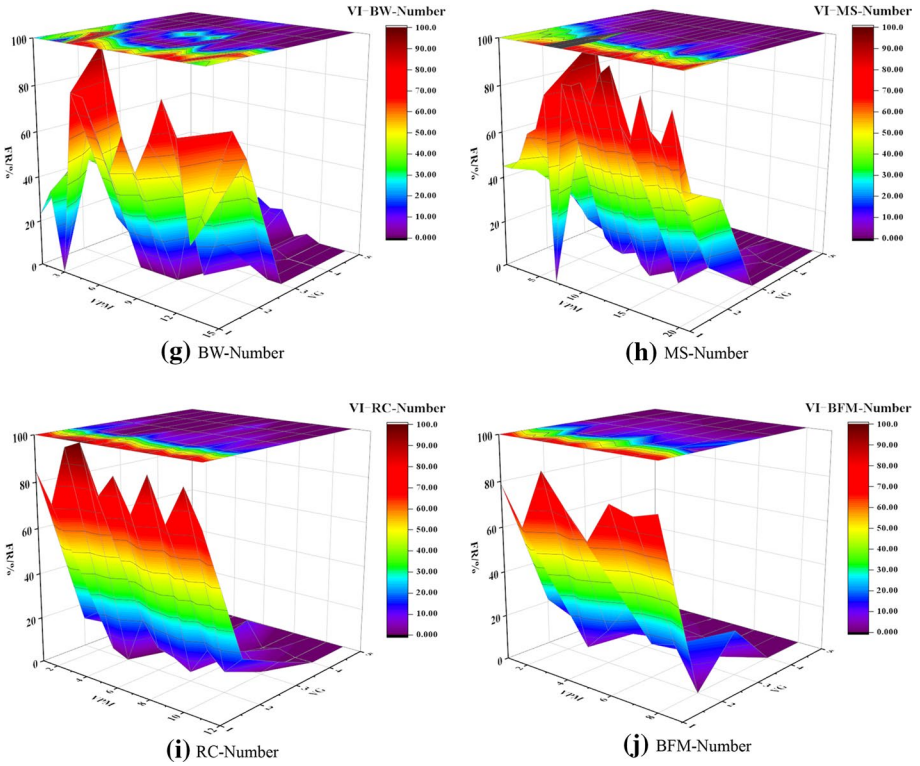

Fig. 9 (continued)

type of structure is relatively heavy in the high-intensity region. The seismic design codes for different structural categories should be considered to increase the flexibility, shear, and compressive capacity between structural members, properly strengthen some structures, improve their lateral force resistance, increase structural measures, and strictly control the construction quality to achieve the goal of improving the seismic capacity of structures.

4.2 Nonlinear vulnerability prediction model of typical structures

Combined with the numerical and probabilistic damage demand model analysis methods, a large number of programs were edited and designed for the actual seismic damage sample points of typical structures. On the premise of fully considering the variance, robustness, regression fit, and prediction regularity, a set of optimized nonlinear regression models (Gaussian first region model (GFRM) and exponential quadratic regression model (EQRM) (Sun et al. 2021; Li and Chen 2020; China Earthquake Administration and National Bureau of Statistics 2005) is proposed to predict the vulnerability of typical structures, as expressed in Eqs. 1–2.

$$FR = m \cdot e^{\left(-\left(\frac{V_{Gn}-n}{p}\right)^2\right)} \tag{1}$$

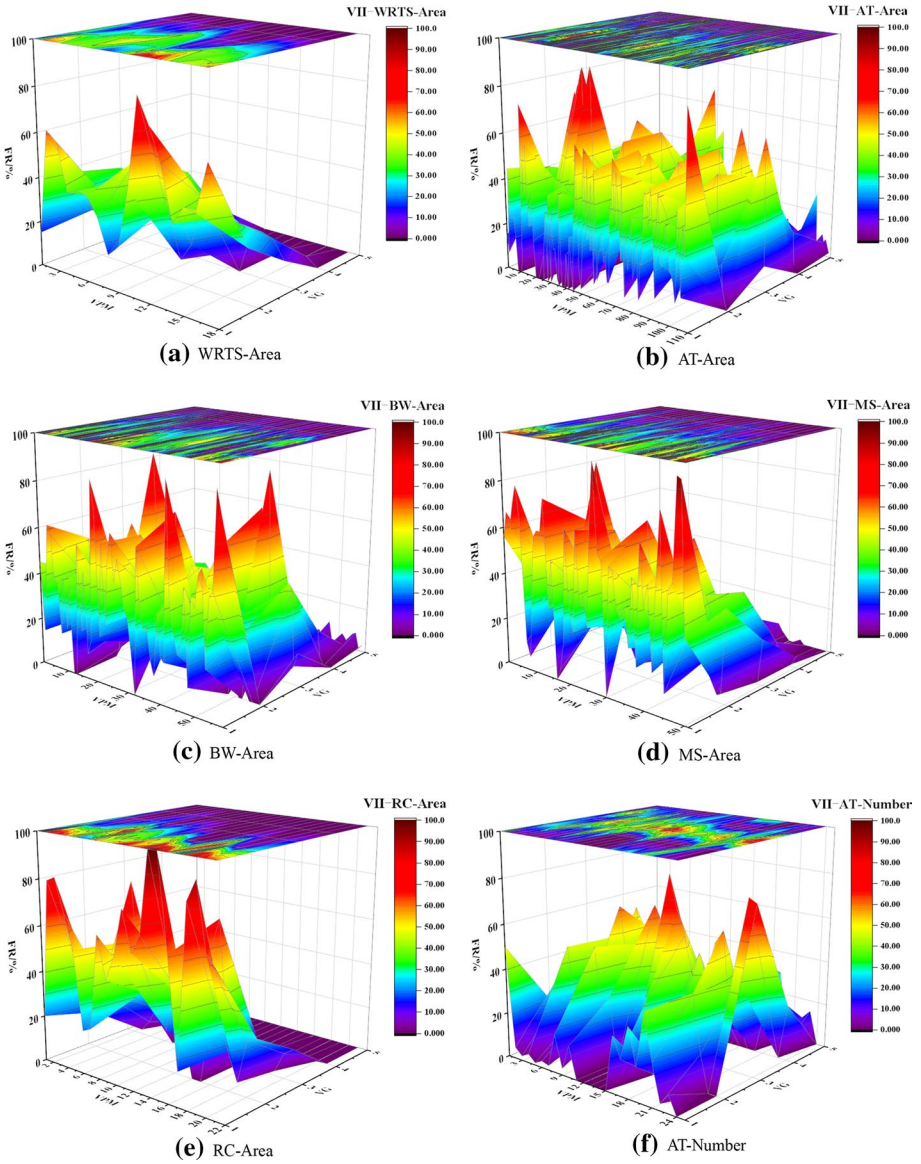

Fig. 10 Vulnerability surface model of the typical structure in degree region of VII

$$FR = a \cdot e^{b \cdot V_{Gn}} + c \cdot e^{d \cdot V_{Gn}} \tag{2}$$

where FR represents the seismic damage failure ratio, V_{Gn} represents the damage states (DSs: DS1, DS2, DS3, DS4, and DS5), and m, n, p, a, b, c, and d represent the undetermined regression parameters of the predicted vulnerability function. A large number of the program editing and significance analyses verified that this group of models could continuously approach the sample data and have the goodness of fit, data significance, variance,

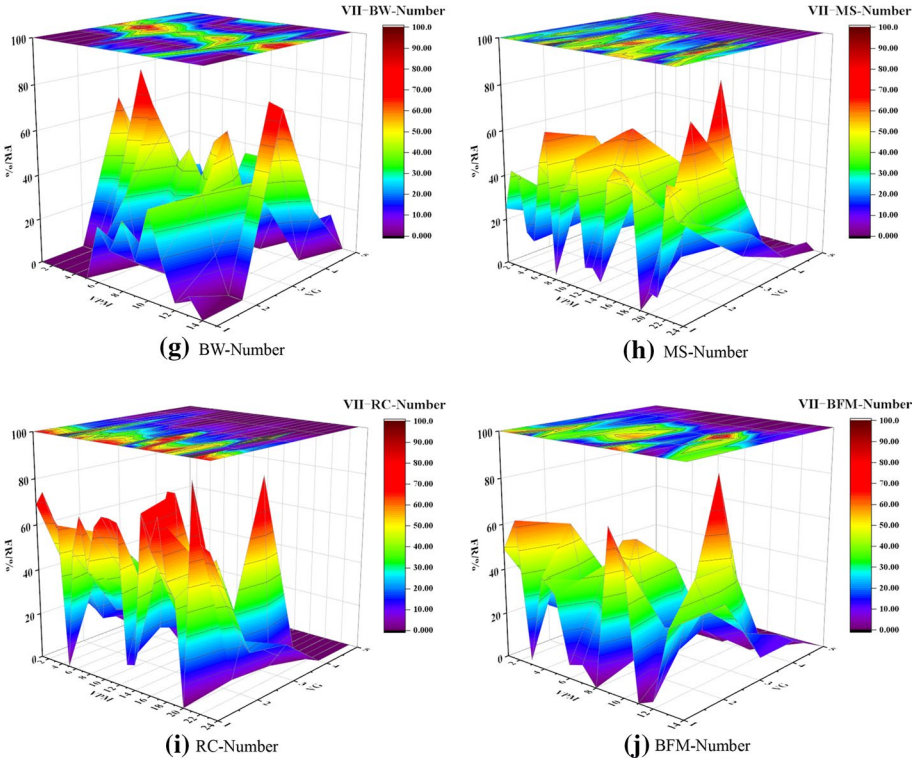

Fig. 10 (continued)

standard deviation, robustness, and regularity. The goodness of fit and data significance parameter (R^2) matrix of the prediction model is developed, as summarized in Table 3.

The nonlinear parameter regression analysis of the actual seismic damage matrix of various typical structures was performed by using the established prediction model. The typical structural vulnerability regression prediction model and parameter matrix based on the investigated area and quantity parameters in different intensity regions were established, as shown in Fig. 14 and Tables 4 and 5 (using the established six types of typical structure sample databases, the parameters of the nonlinear regression model (GFRM and EQRM) were analysed. An optimized comparison model is developed to predict the vulnerability of typical structures in different intensity regions).

To effectively evaluate the average level of vulnerability of various typical structures, 1342 vulnerability matrices are recalculated according to the weighted average method, and the mean probability matrices based on the investigated area and quantity parameters are obtained, as summarized in Tables 6 and 7. The vulnerability curve regression analysis is carried out by using the numerical iterative model theory (shape-preserving (PCHIP) method), and the damage comparison curve model (MVM) is generated, as shown in Fig. 15. The nonlinear vulnerability prediction model (Fig. 14) established based on the actual discrete seismic damage observation samples of six types of structures could be used to predict and evaluate the fragility characteristics of typical structures in different intensity regions. The MVM model (Fig. 15) based on the average matrix of structural vulnerability

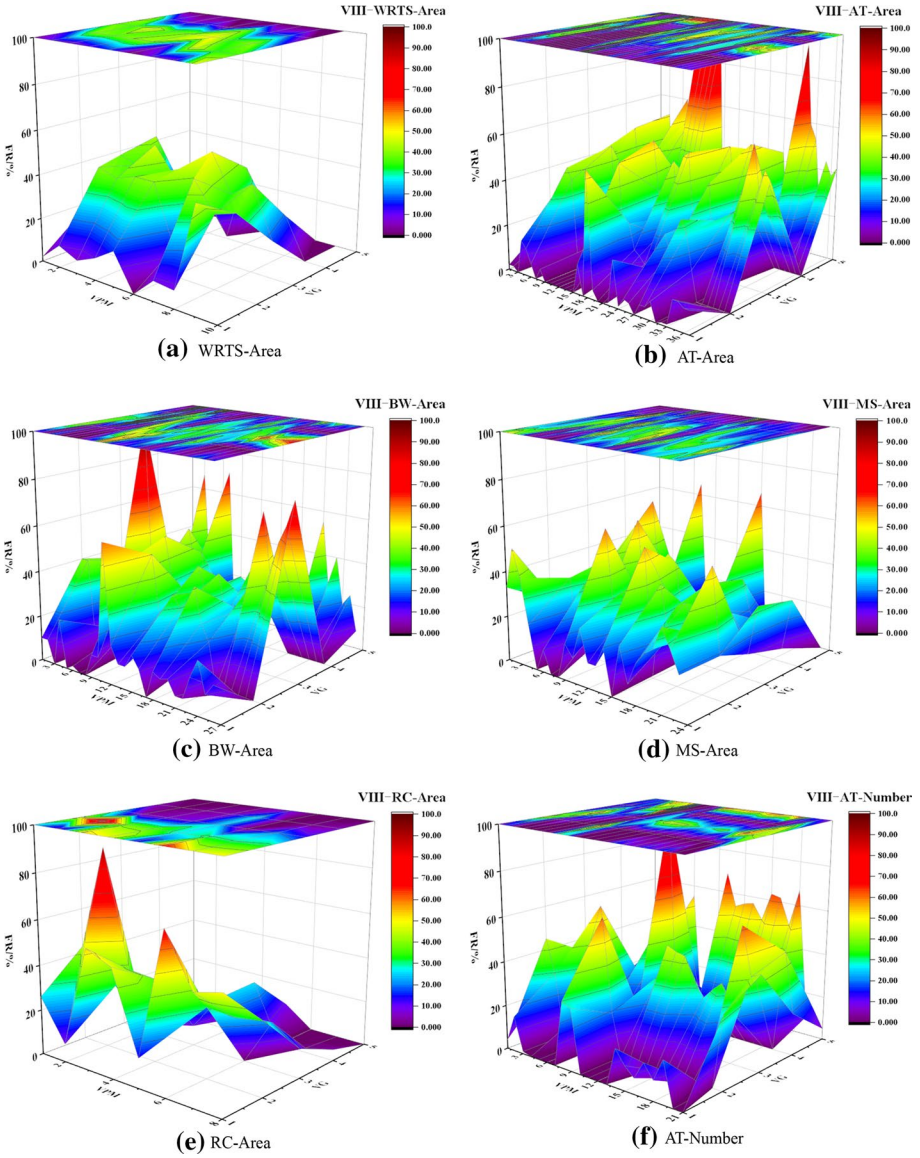

Fig. 11 Vulnerability surface model of the typical structure in degree region of VIII

is more suitable to predict and evaluate the average level of typical structures in multiple intensity regions. The above two models have obvious differences in the objective of predicting and evaluating the vulnerability of typical structures. It is worth noting that the similarity between the nonlinear regression model and the MVM of typical structures is high, which verifies the fitting accuracy of the prediction models (GFRM and EQRM) to a certain extent, especially in the low-intensity region (Figs. 14a and 15a). The accuracy of the vulnerability prediction model of six types of structures is the highest. The predicted

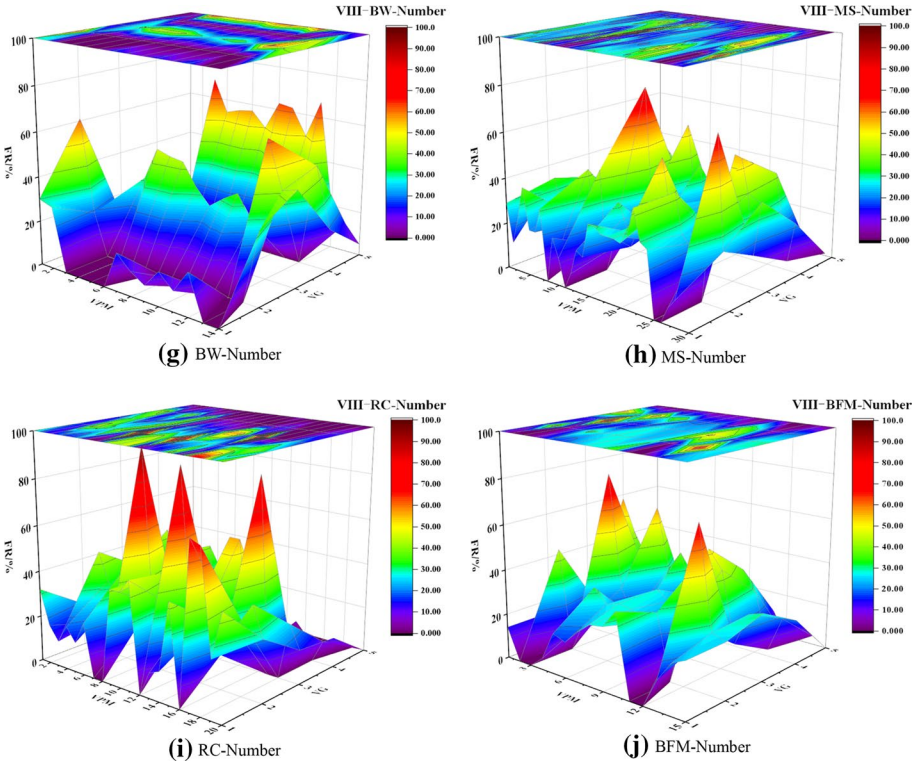

(g) BW-Number **(h)** MS-Number **(i)** RC-Number **(j)** BFM-Number

Fig. 11 (continued)

comparison model curves show that most structural categories follow FR monotonically decreasing as VG increases in low-intensity regions, FR monotonically increasing as VG increases in high-intensity regions, and the gentle change (nonmonotonic or irregular) in medium–high intensity regions (VIII–IX).

However, individual structural categories show abnormal phenomena in the typical intensity region (AT/BW-VII-Number), which is closely related to the seismic capacity of their structural system. According to the sorting results of AT and BW seismic damage observation data in VII region, the spatial distribution of samples surveyed by quantitative parameters is mostly in rural and poor areas, and the economic development is relatively backwards. Most structures are not considered for seismic design, which leads to the insufficient seismic capacity of the above two types of structures. There are relatively many samples of DS3 grade in this intensity area, resulting in abnormal phenomena.

To evaluate the vulnerability characteristics of typical structures in multiple dimensions, combined with the analysis method of the conditional probability calculation model, this study proposes the exceedance probability (EP) damage assessment and prediction function model based on the quantification of different vulnerability levels, as expressed in Eq. 3:

$$P(\mathrm{ES}_i|SID = SID_{i|j}) = P(p \geq p_{i|j}\,|SID = SID_{i|j}) \tag{3}$$

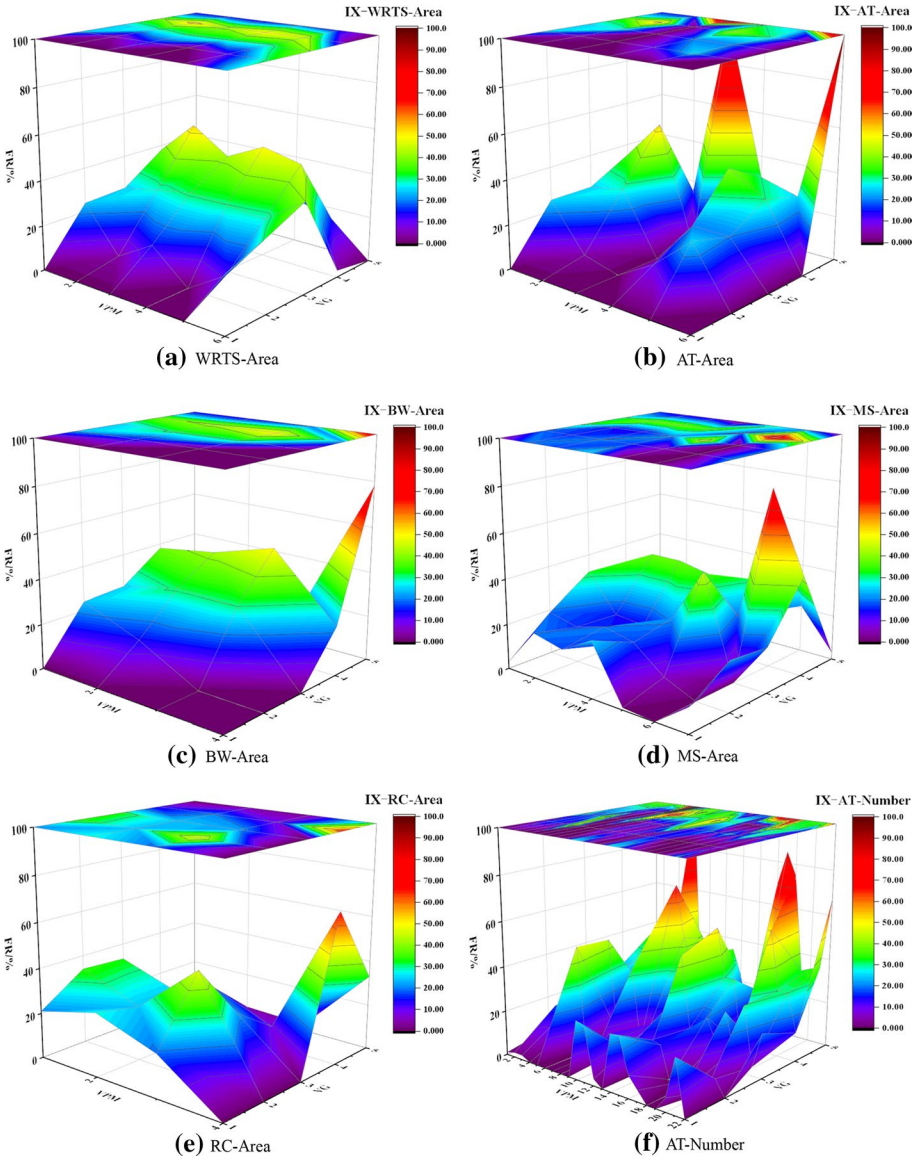

Fig. 12 Vulnerability surface model of the typical structure in degree region of IX

ES_i represents the limit state of the i-th seismic damage states (DSs), SID represents the macroseismic intensity demand (CSIS-20), $SID_{i|j}$ and $p_{i|j}$ represent the intensity demand and probability of the i-th damage (vulnerability levels/(DSs)) of the structure in the j-th intensity region, respectively ($i \in [1,5], j \in [6,11]$), and $P()$ represents the cumulative probability distribution function.

The traditional vulnerability function model of EP and the intensity measure could effectively analyse the relationship between ground motion parameters (PGA and PGV)

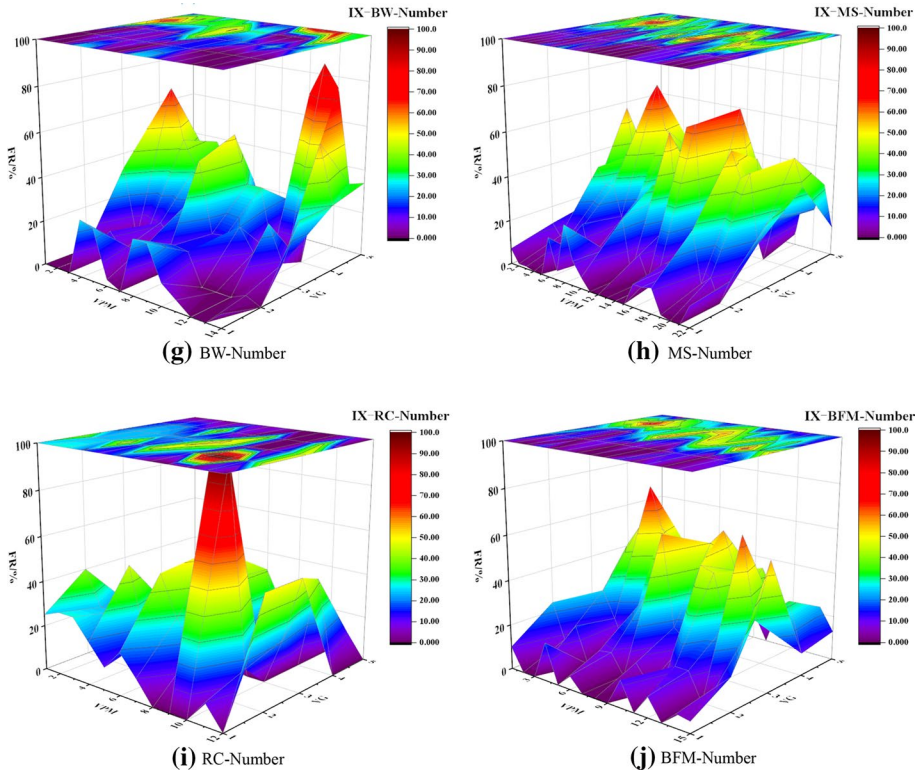

Fig. 12 (continued)

and EP. In this study, a new vulnerability prediction model based on DSs and EP parameters is proposed by using the macroseismic intensity scale (CSIS-20). The model could effectively and intuitively predict and evaluate the variation law of the cumulative exceedance probability under different vulnerability levels.

The 1342 vulnerability probability matrices established based on the investigated area and quantity parameters are calculated by weighted averaging according to the structural category, the cumulative exceedance probability distribution function model is used to numerically calculate the average seismic damage matrix of typical structures in different intensity regions, and the cumulative exceedance probability parameter matrix of six types of structures is established, as indicated in Table 8.

The vulnerability prediction model of typical structures based on EP and DS parameters is developed using the assessment and prediction function model (Eq. 3), the cumulative exceedance probability parameter matrix, numerical iterative model theory (Shape-preserving (PCHIP) method), and probabilistic model analysis method, as reported in Fig. 16.

According to the multidimensional parameter analysis of typical structural vulnerability models (prediction model, mean probability model, and EP model) in different intensity regions, in the degree region of VI, the prediction models of various structures have a slight difference. The damage of AT and BW structures is relatively heavy, and the damage of WRTS and MS is similar. It is worth noting that the DS2 grade of WRTS accounts for a large proportion of the mean model under quantitative parameters, which indicates that

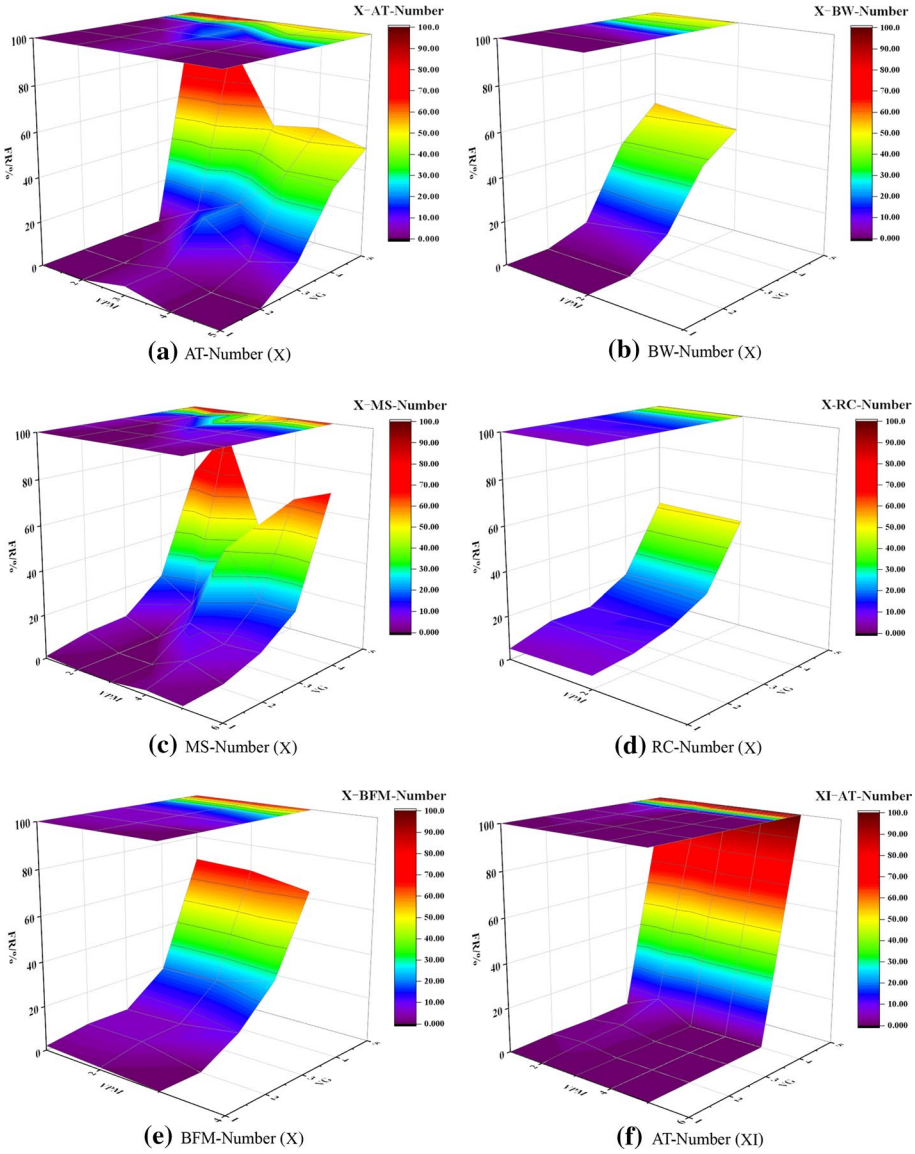

Fig. 13 Vulnerability surface model of the typical structure in degree region of X and XI

such structures are prone to slight earthquake damage in low-intensity regions to a certain extent. The EP of the RC structure at the DS1 level increases significantly. The increase in BFM and MS is relatively fast, indicating that these three structures show good seismic capacity in this intensity region.

In the degree VII region, AT and BW of seismic damage are further aggravated, especially in predicting the quantitative parameter and mean value model and reaching the peak at the DS3 level. MS and BFM seismic damage are relatively close, and the increase of

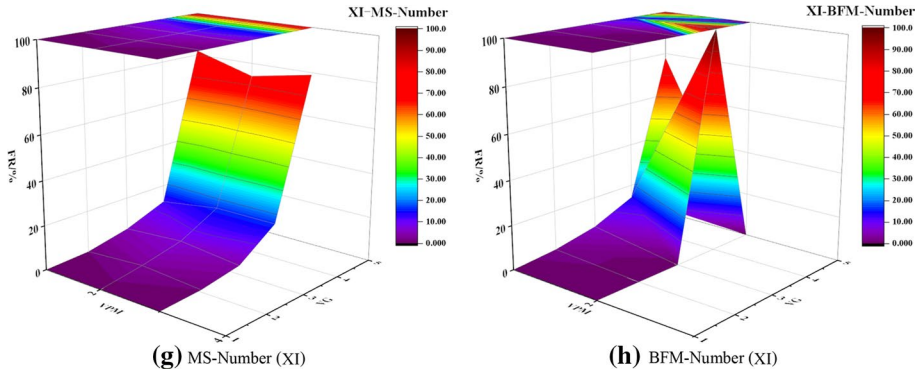

(g) MS-Number (XI) **(h)** BFM-Number (XI)

Fig. 13 (continued)

EP of BFM in DS2 level is slower than MS, indicating that the seismic damage is slightly heavier than MS to a certain extent. We should pay more attention to the seismic defense capacity of AT and BW, design and construct in strict accordance with the structural seismic design code, and appropriately increase reinforcement and structural measures to ensure the seismic capacity in the low-intensity region.

In the degree region of VIII, AT and BW have a high probability of earthquake damage at the DS4 and DS5 levels. The actual earthquake damage mean value model shows that a certain proportion of AT, BW, and MS samples have severe earthquake damage, the failure probability of BFM is significant at the DS4 level, the EP increase of RC at the DS1–DS2 level is low, and the intensity slows down, but it can still reach an EP of 0.8–0.9 at the DS3 level. In the degree region of IX, the peak values of the MS, WRTS, and BW prediction and mean damage models are at the DS4–DS5 level, the damage of MS and BFM are relatively close, and a large proportion of samples are at the DS4 level. In the EP model, AT and BW are the most severely damaged, the surge of WRTS, MS, and BFM curves are similar, and the RC structure still has a large DS3 level of EP. In the degree regions X and XI, the multiple parameter model analysis results show that all structures have severe earthquake damage and that almost all collapse. The BFM prediction model indicates peaks at the DS4 and DS5 levels. The actual damage mean model analysis results verify this prediction conclusion. It is worth noting that the prediction, mean value, and EP model analysis of RC structures in different intensity regions show excellent seismic capacity. Even in the extreme earthquake region, some cases where local or overall failure does not occur. The necessary measures to improve the seismic capacity of various structures should be reasonably set for different intensity regions, especially the seismic design of AT and BW in medium and low-intensity regions, and the application of RC structures should be reasonably popularized.

4.3 A vulnerability predicting matrix model of typical structures by updating the mean vulnerability index

To grasp the seismic vulnerability of regional group structures relatively accurately, the seismic damage (vulnerability) index is widely used in the seismic field of international engineering structures.

Table 3 Goodness of fit and data significance parameter matrix in multiple intensity regions (R^2)

Typical structures	Intensity regions	R^2 (Area)	Prediction model (Area)	R^2 (Number)	Prediction model (Number)
WRTS	VI	0.9412	GFRM	0.9944	GFRM
	VII	0.7049	GFRM	–	–
	VIII	0.6253	GFRM	–	–
	IX	0.5782	EQRM	–	–
AT	VI	0.6152	GFRM	0.5668	GFRM
	VII	0.2573	GFRM	0.3193	GFRM
	VIII	0.1756	GFRM	0.1710	GFRM
	IX	0.3885	EQRM	0.3745	GFRM
	X	1.0000	EQRM	0.8196	GFRM
	XI	–	–	0.9941	EQRM
BW	VI	0.6569	GFRM	0.5328	GFRM
	VII	0.4049	GFRM	0.4978	GFRM
	VIII	0.1419	GFRM	0.1593	GFRM
	IX	0.4587	GFRM	0.3597	EQRM
	X	–	–	0.9932	GFRM
MS	VI	0.7584	GFRM	0.7871	GFRM
	VII	0.5872	GFRM	0.4663	GFRM
	VIII	0.2147	GFRM	0.3346	EQRM
	IX	0.4413	EQRM	0.4931	GFRM
	X	–	–	0.9073	GFRM
	XI	–	–	0.9946	EQRM
RC	VI	0.9202	GFRM	0.9715	EQRM
	VII	0.7087	GFRM	0.6116	GFRM
	VIII	0.5996	GFRM	0.3121	GFRM
	IX	0.0755	GFRM	0.3134	GFRM
	X	–	–	0.9960	EQRM
	XI	–	–	0.9998	EQRM
BFM	VI	0.9995	EQRM	0.8297	EQRM
	VII	–	–	0.4141	GFRM
	VIII	–	–	0.3396	EQRM
	IX	–	–	0.5450	GFRM
	X	–	–	0.9897	EQRM
	XI	–	–	0.4511	GFRM

Kassem et al. (2021), Lagomarsino et al. (2021), and D'Amico et al. (2016) used EMS-98 or MMI standards to divide the seismic damage level. Taking a particular type of typical structure as the research background, they proposed the calculation model of the average seismic damage level and vulnerability index, as expressed in Eq. 4:

$$\mu_{\mathrm{D}} = \mathrm{m}\left[1 + \mathrm{ntanh}\left(\frac{1 + \mathrm{p} \times \mathrm{SVI} - \mathrm{v}}{\mathrm{Q}}\right)\right] \tag{4}$$

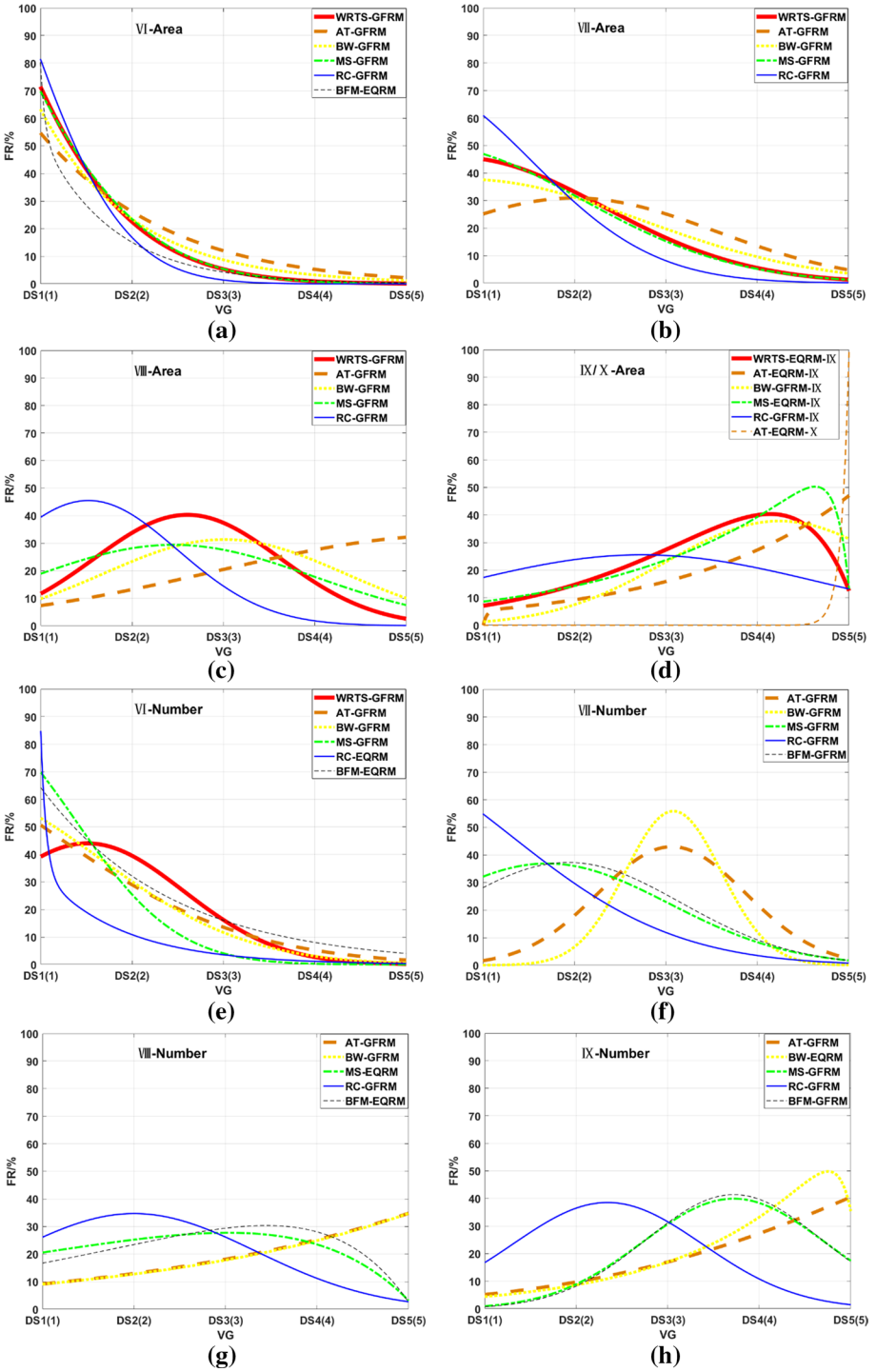

Fig. 14 Vulnerability prediction model curve of typical structures in the multiple intensity regions

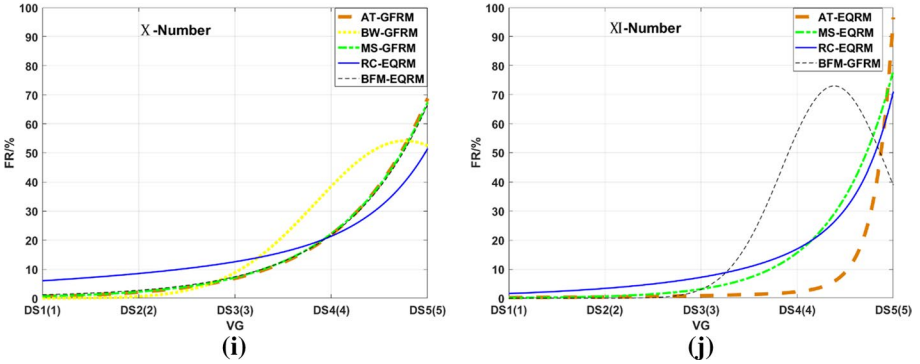

Fig. 14 (continued)

Table 4 Prediction damage vulnerability regression parameter matrix of typical structures in multiple intensity regions (Area)

Typical structures	Intensity regions	GFRM			EQRM			
		m	*n*	*p*	*a*	*b*	*c*	*d*
WRTS	VI	423.1	−2.516	2.637	–	–	–	–
	VII	45.7	0.724	2.254	–	–	–	–
	VIII	40.3	2.605	1.441	–	–	–	–
	IX	–	–	–	−7872	1.011	7876	1.011
AT	VI	1.93×10^{4}	−15.41	6.776	–	–	–	–
	VII	30.92	2.001	2.197	–	–	–	–
	VIII	32.92	5.575	3.733	–	–	–	–
	IX	–	–	–	3.115	0.5431	-3.045×10^{12}	−27.07
	X	–	–	–	0	−7.071	6.138×10^{-25}	12.07
BW	VI	6.59×10^{161}	−743.7	388.8	–	–	–	–
	VII	37.73	0.8077	2.724	–	–	–	–
	VIII	31.34	3.009	1.865	–	–	–	–
	IX	37.81	4.237	1.758	–	–	–	–
MS	VI	196.5	−1.315	2.276	–	–	–	–
	VII	50.13	0.3845	2.397	–	–	–	–
	VIII	29.39	2.451	2.183	–	–	–	–
	IX	–	–	–	-4.338×10^{-14}	6.945	5.15	0.5087
RC	VI	159.8	−0.2089	1.473	–	–	–	–
	VII	72.94	0.1959	1.894	–	–	–	–
	VIII	45.5	1.521	1.379	–	–	–	–
	IX	25.54	2.734	2.781	–	–	–	–
BFM	VI	–	–	–	191.1	−1.269	1.901×10^{10}	−20.4

where μ_D represents the average seismic damage level, SVI represents the seismic vulnerability index, Q represents the toughness factor, *m*, *n*, *p,* and *v* represent the undetermined parameters of the model, and the parameters are identified according to the ground

Table 5 Prediction damage vulnerability regression parameter matrix of typical structures in multiple intensity regions (Number)

Typical structures	Intensity regions	GFRM			EQRM			
		m	*n*	*p*	*a*	*b*	*c*	*d*
WRTS	VI	44.01	1.509	1.491	–	–	–	–
AT	VI	85.25	−1.277	3.154	–	–	–	–
	VII	42.99	3.067	1.143	–	–	–	–
	VIII	2.894×10^{4}	47.26	16.3	–	–	–	–
	IX	89.34	9.445	5	–	–	–	–
	X	3.12×10^{14}	56.57	9.553	–	–	–	–
	XI	–	–	–	2.317×10^{-10}	5.343	0.09451	0.7305
BW	VI	63.72	0.03124	2.276	–	–	–	–
	VII	55.92	3.083	0.7418	–	–	–	–
	VIII	1.673×10^{229}	3140	136.9	–	–	–	–
	IX	–	–	–	2.248	0.6736	-3.053×10^{-14}	6.902
	X	54.18	4.766	1.313	–	–	–	–
MS	VI	86.61	0.275	1.558	–	–	–	–
	VII	36.9	1.703	1.886	–	–	–	–
	VIII	–	–	–	1.464×10^{4}	0.4847	-1.463×10^{4}	0.4849
	IX	39.94	3.72	1.406	–	–	–	–
	X	4.306×10^{13}	54.48	9.49	–	–	–	–
	XI	–	–	–	0.0252	1.608	0	−33.74
RC	VI	–	–	–	101.9	−1.121	2.217×10^{9}	−17.59
	VII	78.26	−0.5299	2.571	–	–	–	–
	VIII	34.69	2.001	1.88	–	–	–	–
	IX	38.55	2.342	1.47	–	–	–	–
	X	–	–	–	4.316	0.3311	0.005164	1.726
	XI	–	–	–	1.495×10^{-5}	2.958	0.7585	0.745
BFM	VI	–	–	–	128.5	−0.6931	0	−0.6931

Table 5 (continued)

Typical structures	Intensity regions	GFRM			EQRM			
		m	*n*	*p*	*a*	*b*	*c*	*d*
	VII	37.3	1.931	1.751	–	–	–	–
	VIII	–	–	–	-1.639×10^{4}	0.622	1.64×10^{4}	0.6219
	IX	41.41	3.723	1.356	–	–	–	–
	X	–	–	–	0.2187	1.141	0.4736	0.1512
	XI	72.98	4.386	0.7759	–	–	–	–

Table 6 Mean probability matrix of typical structures in multiple intensity regions (Area)

Structure type	Seismic intensity	Mean failure ratio (%)				
		DS1	DS2	DS3	DS4	DS5
WRTS	VI	72	22	6	0	0
	VII	45	32	19	4	0
	VIII	12	34	37	16	1
	IX	4	14	30	39	13
AT	VI	55	25	14	4	2
	VII	25	31	26	12	6
	VIII	6	11	27	22	34
	IX	0	11	16	26	47
	X	0	0	0	0	100
BW	VI	63	23	10	3	1
	VII	39	27	26	6	2
	VIII	11	19	38	16	16
	IX	0	10	21	38	31
MS	VI	70	24	5	1	0
	VII	47	32	15	6	0
	VIII	18	29	27	18	8
	IX	11	14	21	41	13
RC	VI	82	17	1	0	0
	VII	61	29	8	2	0
	VIII	39	41	13	6	1
	IX	17	26	20	27	10
BFM	VI	80	15	5	0	0

motion parameters or macrointensity in different regions to determine the undetermined parameters.

Polese et al. (2015) and Brando et al. (2017), combined actual survey data of earthquake damage in Italy in 2009, constructed a nonlinear model by using the Monte Carlo model program and proposed using the binomial distribution probability density model in probability theory to establish its vulnerability index (earthquake damage index) function. Ferreira et al. (2013), based on the four elements of the structural system, irregular layout and interaction, height factor and associated mode and 14 types of parameters included, established the calculation model of the seismic damage index, as expressed in Eq. 5:

$$I_v^* = \sum_{i=1}^{14} C_{vi} \times p_i \tag{5}$$

where I_v^* represents the seismic damage index considering 14 types of parameters, C_{vi} represents the structural damage level, and p_i represents the weight of each parameter. The model is used to analyse the vulnerability of more than 500 typical houses in the old urban centre region of Seixal in Portugal based on the seismic damage index, and the vulnerability curves of the average seismic damage index and seismic intensity (EMS-98) are established. Reference (Li et al. 2021a) used CSIS-08, EMS-98, and MSK-81 to analyse the vulnerability of typical structures in the Wenchuan earthquake in China. It analysed

Table 7 Mean probability matrix of a typical structure in multiple intensity regions (Number)

Structure type	Seismic intensity	Mean failure ratio (%)				
		DS1	DS2	DS3	DS4	DS5
WRTS	VI	39	40	15	5	1
AT	VI	51	28	15	3	3
	VII	11	14	45	19	11
	VIII	8	9	31	15	37
	IX	7	8	17	28	40
	X	1	1	8	21	69
	XI	0	1	1	2	96
BW	VI	53	30	13	1	3
	VII	11	7	55	12	15
	VIII	10	8	35	6	41
	IX	9	5	17	33	36
	X	0	0	9	39	52
MS	VI	70	25	4	1	0
	VII	32	35	24	8	1
	VIII	20	26	27	24	3
	IX	5	9	30	39	17
	X	1	3	7	22	67
	XI	0	2	5	15	78
RC	VI	86	10	3	1	0
	VII	54	30	13	3	0
	VIII	25	36	25	13	1
	IX	14	42	22	18	4
	X	5	10	12	22	51
	XI	1	4	7	17	71
BFM	VI	73	20	5	2	0
	VII	29	34	31	6	0
	VIII	14	26	28	29	3
	IX	4	8	29	42	17
	X	2	5	5	20	68
	XI	0	2	6	14	78

the differences of the vulnerability of typical structures under different intensity standards, and (Li et al. 2021b) collected and sorted out BW actual seismic damage observation data in historical earthquakes in China and conducted damage assessment using CSIS-08. However, researchers have studied the vulnerability of a single structural category according to a certain intensity standard, and the damage quantification scales of many intensity standards for structural types are relatively old. It was difficult to effectively quantify and predict the vulnerability characteristics of various group structures.

In this study, the updated mean vulnerability index (UMVI) prediction matrix model, which can be used to evaluate the vulnerability of typical regional structures, is proposed by using the latest version of the China intensity scale (CSIS-20), which is expressed in Eqs. 6–8,

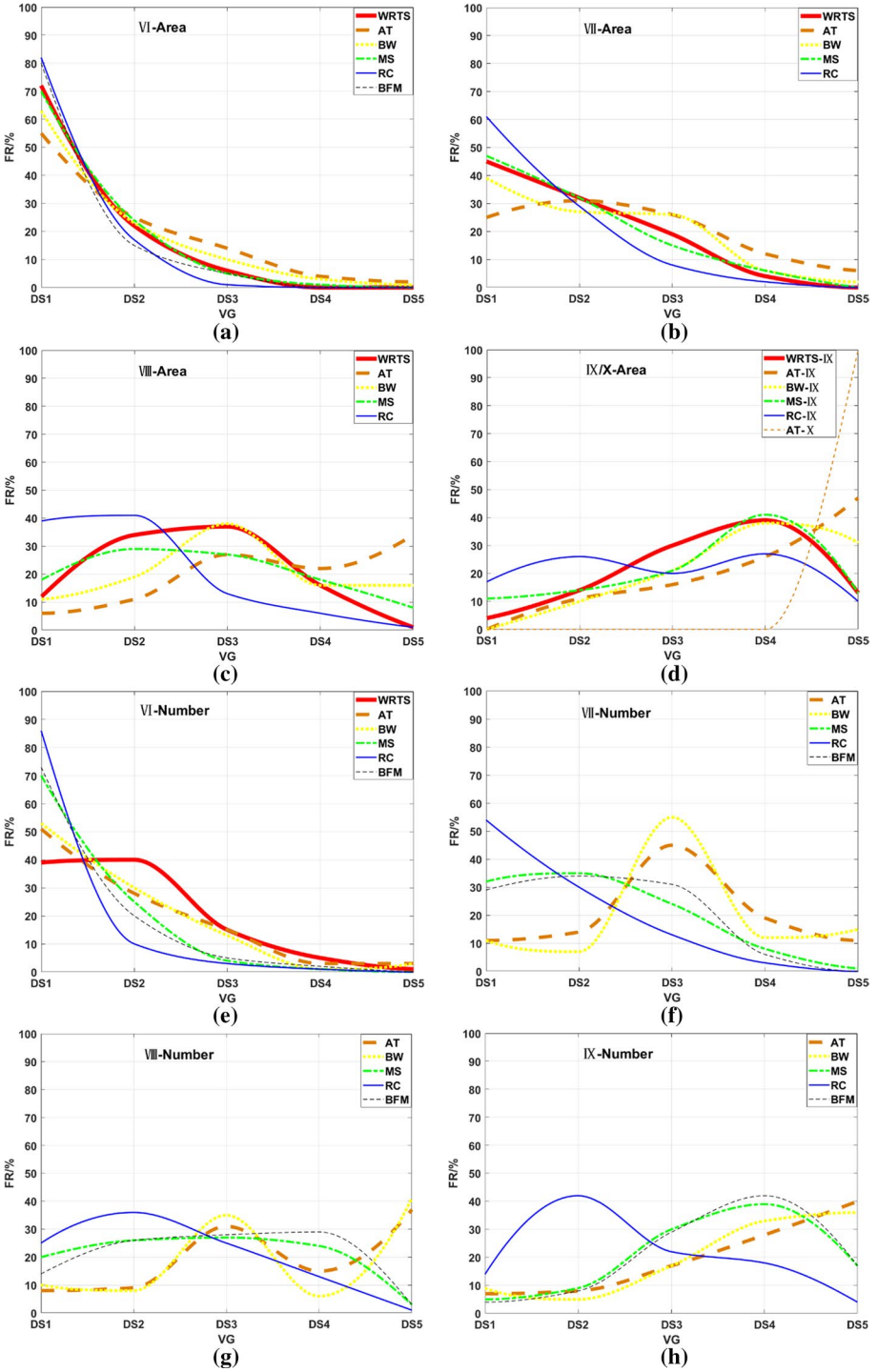

Fig. 15 Mean vulnerability model curve of typical structures in the multiple intensity regions

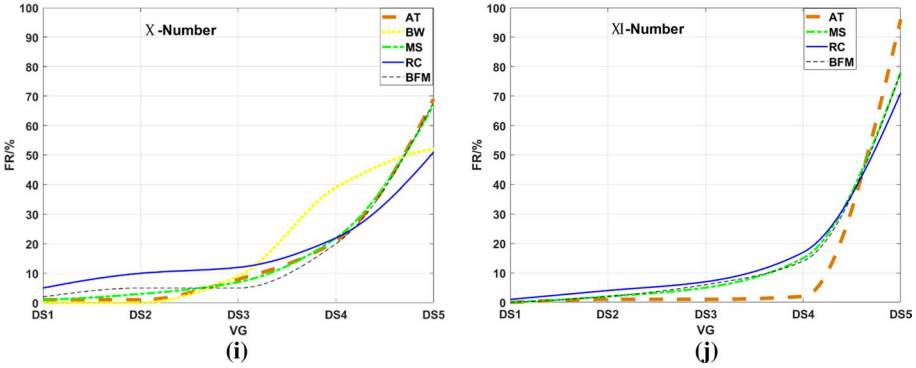

Fig. 15 (continued)

$$[UMVI]_T = [\Xi_{qp}] \times [s_p] \tag{6}$$

$$[UMVI]_T = \begin{bmatrix} \Xi_{61} & \Xi_{62} & \cdots & \cdots & \Xi_{6p} \\ \Xi_{71} & \Xi_{72} & \cdots & \cdots & \Xi_{7p} \\ \Xi_{81} & \Xi_{82} & \cdots & \cdots & \Xi_{8p} \\ \vdots & \vdots & \ddots & & \vdots \\ \vdots & \vdots & & \ddots & \vdots \\ \Xi_{q1} & \Xi_{q2} & \cdots & \cdots & \Xi_{qp} \end{bmatrix} \times \begin{bmatrix} s_1 \\ s_2 \\ \vdots \\ \vdots \\ s_p \end{bmatrix} \tag{7}$$

$$[UMVI]_{T_s} = \begin{bmatrix} UMVI_6 & UMVI_7 & \cdots & \cdots & UMVI_q \end{bmatrix}^{\mathrm{T}} \tag{8}$$

where $s_p$is the seismic damage index of vulnerability grade p, Ξ_{qp} is the structure FR of vulnerability grade p in the q intensity region ($p = 1$, 2, 3, 4, and 5; $q = 7$, 8, 9, 10, and 11), and $[UMVI]_{T_s}$ is the *UMVI* matrix of T-type structure (s is the upper limit (u), mean value (m) and lower limit (d); T-type structure: WRTS, AT, BW, MS, RC, and BFM), as indicated by Table 9. The established actual vulnerability probability matrix and macrointensity level are substituted into the *UMVI* prediction model (Eqs. 6–8) to obtain the vulnerability prediction of three levels (d, m, and u) of typical regional structures.

The *UMVI* is used to evaluate the vulnerability level of all samples in the WRTS, AT, BW, MS, RC, and BFM sample databases. After a substantial number of model calculations and analyses, the prediction vulnerability models and parameter matrices of various typical structures in different intensity regions are established, as shown in Fig. 17 and Table 10. Due to the difference in the highest seismic intensity of WRTS and BW (IX and X), they are analysed separately from other structural types.

According to the established *UMVI* prediction model of typical structures, the seismic damage of WRTS and AT in the overall seismic region is relatively heavy, the damage degree of BFM and MS in multiple intensity regions is similar, the BW damage is slightly lighter than AT, and the seismic damage of RC structure is the lightest. The reliability of the established *UMVI* prediction model is verified by using the actual seismic damage sample data of six types of typical buildings (see supplementary data 2). It can be extended to the vulnerability prediction and evaluation of typical structures in different intensity regions.

Table 8 Cumulative exceedance probability parameter matrix of typical structures in different intensity regions (EP)

Typical structures	Intensity regions	Cumulative exceedance probability parameter (EP) under different vulnerability levels				
		DS1	DS2	DS3	DS4	DS5
WRTS	VI	0.7	0.93	0.99	1	1
	VII	0.45	0.77	0.96	1	1
	VIII	0.12	0.46	0.83	0.99	1
	IX	0.04	0.18	0.48	0.87	1
AT	VI	0.54	0.8	0.94	0.98	1
	VII	0.23	0.5	0.8	0.93	1
	VIII	0.06	0.17	0.46	0.65	1
	IX	0.06	0.14	0.31	0.58	1
	X	0	0.01	0.08	0.26	1
	XI	0	0.01	0.02	0.04	1
BW	VI	0.63	0.86	0.96	0.99	1
	VII	0.33	0.56	0.88	0.96	1
	VIII	0.11	0.26	0.63	0.76	1
	IX	0.07	0.13	0.31	0.65	1
	X	0	0	0.09	0.48	1
MS	VI	0.7	0.94	0.99	1	1
	VII	0.42	0.75	0.93	0.99	1
	VIII	0.2	0.47	0.74	0.95	1
	IX	0.07	0.17	0.45	0.84	1
	X	0.01	0.04	0.11	0.33	1
	XI	0	0.02	0.07	0.22	1
RC	VI	0.82	0.98	1	1	1
	VII	0.58	0.88	0.98	1	1
	VIII	0.29	0.66	0.88	0.99	1
	IX	0.14	0.51	0.73	0.94	1
	X	0.05	0.15	0.27	0.49	1
	XI	0.01	0.05	0.12	0.29	1
BFM	VI	0.75	0.94	0.99	1	1
	VII	0.35	0.69	0.94	1	1
	VIII	0.14	0.4	0.68	0.97	1
	IX	0.04	0.12	0.41	0.83	1
	X	0.02	0.07	0.12	0.32	1
	XI	0	0.02	0.08	0.22	1

5 Conclusion

Building structures show different seismic damage characteristics under earthquakes of varying intensity levels. In-depth study of the seismic vulnerability of typical structures is of engineering significance to building loss assessment, prediction, and seismic design. This study carried out a field investigation to accurately grasp the vulnerability characteristics of typical structures under different intensity levels. Seismic vulnerability

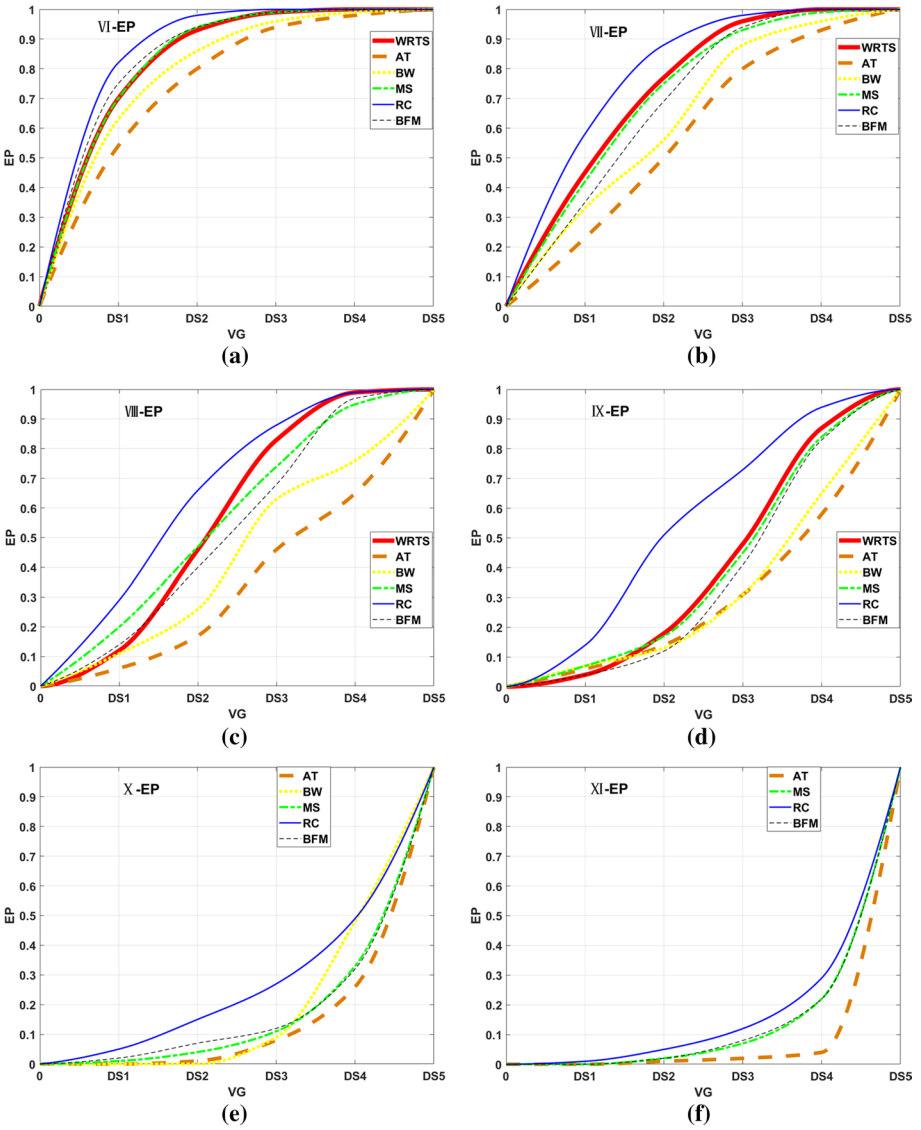

Fig. 16 Exceedance probability prediction model curve of typical structures in the multiple intensity regions

Table 9 Vulnerability grade and *s* interval (CSIS-20)

VG	Median	Value interval
DS1	0.05	$0.00 \le s < 0.10$
DS2	0.20	$0.10 \le s < 0.30$
DS3	0.43	$0.30 \le s < 0.55$
DS4	0.70	$0.55 \le s < 0.85$
DS5	0.93	$0.85 \le s \le 1.00$

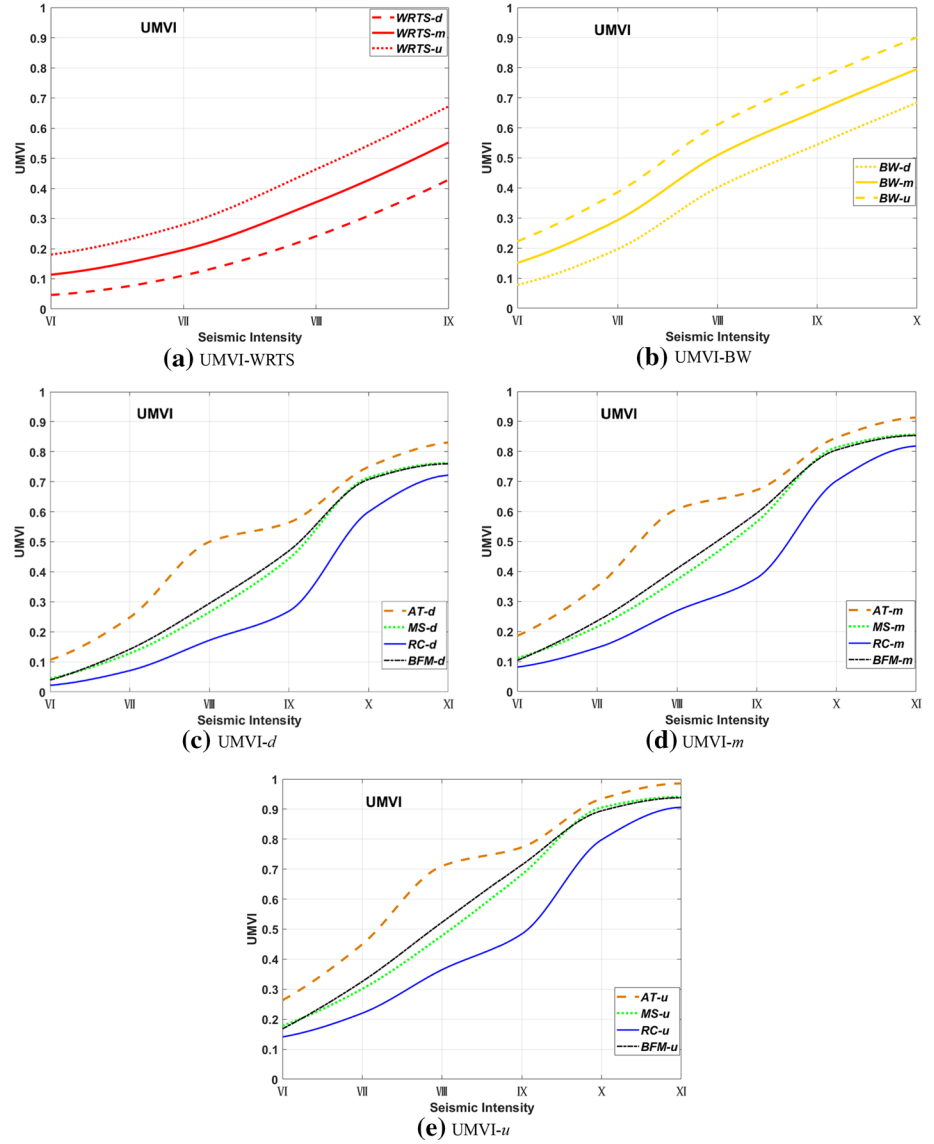

Fig. 17 Vulnerability prediction model of typical structures considering UMVI

analysis on six types of structures (wood roof truss structure (WRTS), adobe and timber (AT) structure, brick wood (BW) structure, masonry structure (MS), RC structure, and bottom frame seismic wall masonry structure (BFM)) widely used worldwide, a model for evaluating and predicting the vulnerability of the above structures is established and proposed. The structural vulnerability is compared and analysed combined with the established actual earthquake damage observation database. The results are as follows:

Table 10 Parameter model based on UMVI

Type	Parameter	Intensity					
		VI	VII	VIII	IX	X	XI
WRTS	*d*	0.0465	0.111	0.2415	0.429	–	–
	m	0.1138	0.1962	0.3544	0.5529	–	–
	u	0.1805	0.2795	0.4635	0.6725	–	–
AT	*d*	0.107	0.248	0.5	0.5645	0.75	0.831
	m	0.1858	0.3506	0.6082	0.6717	0.8463	0.9131
	u	0.263	0.4495	0.71	0.773	0.9345	0.9855
BW	*d*	0.078	0.197	0.4015	0.5445	0.6835	–
	m	0.1508	0.2933	0.5088	0.6564	0.7953	–
	u	0.2225	0.386	0.61	0.763	0.901	–
MS	*d*	0.0445	0.1285	0.266	0.4445	0.7145	0.7625
	m	0.1115	0.2157	0.3736	0.5657	0.8137	0.8559
	u	0.178	0.301	0.478	0.6825	0.9055	0.941
RC	*d*	0.022	0.071	0.172	0.2695	0.6005	0.722
	m	0.0816	0.146	0.2694	0.3784	0.7024	0.8179
	u	0.141	0.22	0.3645	0.4845	0.798	0.906
BFM	*d*	0.0395	0.142	0.295	0.4705	0.708	0.76
	m	0.104	0.235	0.4103	0.5948	0.8049	0.8532
	u	0.168	0.3255	0.5225	0.7145	0.8945	0.938

1. We collected statistics and sorted the structural investigation data ($98{,}051.8122 \times 10^4$ m^2 and 995,269 buildings) of 213 destructive earthquakes in China from 1975 to 2013. The vulnerability of the actual seismic damage observation data of six types of structures is evaluated. The actual seismic damage sample database based on typical structures is established using the latest China seismic intensity scale (CSIS-20).
2. Combined with the field damage inspection of typical structures, the actual seismic damage characteristics and mechanism of WRTS, AT, BW, MS, RC, and BFM are analysed, and measures and methods to improve the seismic capacity of various structures are proposed.
3. A substantial number of statistical studies have been performed on earthquake damage observations in 23 provinces (autonomous regions and municipalities directly under the central government) in China. The statistical analysis of the investigation area and quantity under the influence of region, age, and frequency is provided. It is observed that the AT and BW are significantly greater than other structural categories; earthquakes affecting the structure occurred more frequently in 2003 and 2008.
4. Based on the principles of mathematical statistics and risk analysis, the field observation sample data of buildings are analysed and processed, 1342 typical structural vulnerability matrices and vulnerability surface models based on FR parameters are established, and a comparison of the vulnerability seismic damage characteristics of structures in multiple intensity regions is provided for different structural types. It is observed that the vulnerability of RC buildings is the weakest, and it shows excellent seismic performance in different intensity regions. A large number of MSs and ATs after seismic design can still ensure no serious damage or collapse in medium- to high-intensity regions.

5. The optimized nonlinear prediction regression model and EP probability model, which can be used to evaluate and predict the vulnerability of typical structures, are proposed. A significant amount of model analysis work is conducted, and the vulnerability prediction comparison model and EP model of typical structures based on the investigated area and quantity are established. The calculation method of the regional group structure vulnerability prediction matrix model with the UMVI parameter is proposed, and the vulnerability comparison model of typical structures is established combined with CSIS-20. The analysis results are in good agreement with the actual earthquake damage observations.

In this study, the vulnerability prediction and evaluation model of typical structures established has a certain application value after being verified by a large number of actual earthquake damage observation data. It can be extended to the vulnerability prediction and evaluation of typical structures in different intensity regions and provide a necessary reference for future seismic design and intensity standard revision.

Supplementary Information The online version contains supplementary material available at https://doi.org/10.1007/s10518-022-01395-y.

Acknowledgements The basic data of this study were derived from the seismic damage investigation database of the China Earthquake Administration (CAE) and the Wenchuan earthquake damage investigation team of the Institute of Engineering Mechanics of CAE. I would like to express my sincere gratitude to them. In addition, the research described in this paper was financially supported by the Basic Scientific Research Business Expenses of Provincial Universities in Heilongjiang Province (2021-KYYWF-0044) and Key Laboratory of Functional Inorganic Material Chemistry (Heilongjiang University), Ministry of Education.

Funding The authors have not disclosed any funding.

Declarations

Conflict of interest The authors have not disclosed any competing interest.

References

Altindal A, Karimzadeh S, Erberik MA, Askan A, Anil O, Kockar MK, Sahmaran M (2021) A case study for probabilistic seismic risk assessment of earthquake-prone old urban centers. IInt J Disaster Risk Reduc 61:102376. https://doi.org/10.1016/j.ijdrr.2021.102376

Avila-Haro JA, Gonzalez-Drigo R, Vargas-Alzate YF, Pujades L, Barbat A (2022) Probabilistic seismic assessment of a high-rise URM building. J Build Eng 45:103344. https://doi.org/10.1016/j.jobe.2021.103344

Biglari M, Formisano A, Hashemi BH (2021) Empirical fragility curves of engineered steel and RC residential buildings after Mw 7.3 2017 Sarpol-e-zahab earthquake. Bull Earthq Eng 19:2671–2689. https://doi.org/10.1007/s10518-021-01090-4

Biglari M, Formisano A, Davino A (2022) Seismic vulnerability assessment and fragility analysis of Iranian historical mosques in Kermanshah city. J Build Eng 45:103673. https://doi.org/10.1016/j.jobe.2021.103673

Bilgin H, Shkodrani N, Hysenlliu M, Ozmen HB, Isik E, Harirchian E (2022) Damage and performance evaluation of masonry buildings constructed in 1970s during the 2019 Albania earthquakes. Eng Fail Anal 131:105824. https://doi.org/10.1016/j.engfailanal.2021.105824

Brando G, De-Matteis G, Spacone E (2017) Predictive model for the seismic vulnerability assessment of small historic centres: application to the inner Abruzzi region in Italy. Eng Struct 153:81–96. https://doi.org/10.1016/j.engstruct.2017.10.013

Brando G, Cianchino G, Rapone D, Spacone E, Biondi S (2021) A CARTIS-based method for the rapid seismic vulnerability assessment of minor Italian historical centres. Int J Disaster Risk Reduct 63:102478. https://doi.org/10.1016/j.ijdrr.2021.102478

Briceño C, Noel MF, Chácara C, Aguilar R (2021) Integration of non-destructive testing, numerical simulations, and simplified analytical tools for assessing the structural performance of historical adobe buildings. Constr Build Mater 290:123224. https://doi.org/10.1016/j.conbuildmat.2021.123224

Chen H, Xie QC, Li ZQ, Xue W, Liu K (2017) Seismic damage to structures in the 2015 Nepal earthquake sequences. J Earthquake Eng 21(4):551–578. https://doi.org/10.1080/13632469.2016.1185055

Chieffo N, Mosoarca M, Formisano A, Lourenço PB, Milani G (2021) The effect of ground motion vertical component on the seismic response of historical masonry buildings: the case study of the Banloc Castle in Romania. Eng Struct 249:113346. https://doi.org/10.1016/j.engstruct.2021.113346

China Earthquake Administration and National Bureau of Statistics (1996) Compilation of loss assessment for earthquake disasters in mainland China (1990–1995). Earthquake Press, Beijing

China Earthquake Administration and National Bureau of Statistics (2001) Compilation of loss assessment for earthquake disasters in mainland China (1996–2000). Earthquake Press, Beijing

China Earthquake Administration and National Bureau of Statistics (2005) Compilation of loss assessment for earthquake disasters in mainland China (2001–2005). Earthquake Press, Beijing

Clarke R, Carey B (2021) Seismic fragility functions for a pervasive unique form of construction with very high potential for social losses in Trinidad and Tobago: two-story houses. Earthq Spectra. https://doi.org/10.1177/87552930211047258

D'Amico S, Meroni F, Sousa ML, Zonno G (2016) Building vulnerability and seismic risk analysis in the urban area of Mt. Etna volcano (Italy). Bull Earthq Eng 14(7):2031–2045. https://doi.org/10.1007/s10518-015-9804-4

Dai JW, Chen JG, Zhang CX, Nie GB, Liu YB (2020) Seismic damage investigation and seismic performance study of Lushan middle school gymnasium. J Perform Constr Facil 34(3):04020041. https://doi.org/10.1061/(ASCE)CF.1943-5509.0001431

Domaneschi M, Noori AZ, Pietropinto MV, Cimellaro GP (2021) Seismic vulnerability assessment of existing school buildings. Comput Struct 248:106522. https://doi.org/10.1016/j.compstruc.2021.106522

Eudave RR, Ferreira TM (2021) On the potential of using the Mexican National Catalogue of Historical Monuments for assessing the seismic vulnerability of existing buildings: a proof-of-concept study. Bull Earthq Eng 19(12):4945–4978. https://doi.org/10.1007/s10518-021-01154-5

Ferreira TM, Vicente R, Mendes JAR, Varum H, Costa A (2013) Seismic vulnerability assessment of historical urban centres: case study of the old city centre in Seixal, Portugal. Bull Earthquake Eng 11(5):1753–1773. https://doi.org/10.1007/s10518-013-9447-2

Gaudio CD, Scala SA, Ricci P, Verderame GM (2021) Evolution of the seismic vulnerability of masonry buildings based on the damage data from L'Aquila 2009 event. Bull Earthq Eng 19(11):4435–4470. https://doi.org/10.1007/s10518-021-01132-x

Godínez-Domínguez EA, Tena-Colunga A, Pérez-Rocha LE, Archundia-Aranda HI, Bernal AG, Ruiz-Torres RPR (2021) The September 7, 2017 Tehuantepec, Mexico, earthquake: damage assessment in masonry structures for housing. Int J Disaster Risk Reduct 56:102123. https://doi.org/10.1016/j.ijdrr.2021.102123

Grigoratos L, Monteiro R, Ceresa P, Meo AD, Faravelli M, Borzi B (2021) Crowdsourcing exposure data for seismic vulnerability asessment in developing countries. J Earthquake Eng 25(5):835–852. https://doi.org/10.1080/13632469.2018.1537901

Halder L, Dutta SC, Sharma RP, Bhattacharya S (2021) Lessons learnt from post-earthquake damage study of Northeast India and Nepal during last ten years: 2021 Assam earthquake, 2020 Mizoram earthquake, 2017 Ambasa earthquake, 2016 Manipur earthquake, 2015 Nepal earthquake, and 2011 Sikkim earthquake. Soil Dyn Earthq Eng 151:106990. https://doi.org/10.1016/j.soildyn.2021.106990

Kassem MM, Nazri FM, Farsangi EN, Tan CG (2021) Comparative seismic RISK assessment of existing RC buildings using seismic vulnerability index approach. Structures 32:889–913. https://doi.org/10.1016/j.istruc.2021.03.032

Kechidi S, Castro JM, Monteiro R, Marques M, Yelles K, Bourahla N, Hamdache M (2021) Development of exposure datasets for earthquake damage and risk modelling: the case study of northern Algeria. Bull Earthq Eng 19(12):5253–5283. https://doi.org/10.1007/s10518-021-01161-6

Kita A, Cavalagli N, Venanzi I, Ubertini F (2021) A new method for earthquake-induced damage identification in historic masonry towers combining OMA and IDA. Bull Earthq Eng 19(12):5307–5337. https://doi.org/10.1007/s10518-021-01167-0

Lagomarsino S, Cattari S, Ottonelli D (2021) The heuristic vulnerability model: fragility curves for masonry buildings. Bull Earthq Eng 19(8):3129–3163. https://doi.org/10.1007/s10518-021-01063-7

Li SQ, Chen YS (2020) Analysis of the probability matrix model for the seismic damage vulnerability of empirical structures. Nat Hazards 104(1):705–730. https://doi.org/10.1007/s11069-020-04187-2
Li SQ, Yu TL, Chen YS (2019) Comparative analysis of the empirical seismic vulnerability of typical structures in multiple intensity zone. Arch Civ Eng 65(3):167–183. https://doi.org/10.2478/ace-2019-0042
Li SQ, Chen YS, Yu TL (2021a) Comparison of macroseismic intensity scales by considering empirical observations of structural seismic damage. Earthq Spectra 37(1):449–485. https://doi.org/10.1177/8755293020944174
Li SQ, Liu HB, Chen YS (2021b) Vulnerability models of brick and wood structures considering empirical seismic damage observations. Structures 34:2544–2565. https://doi.org/10.1016/j.istruc.2021.09.023
Lovon H, Silva V, Vicente R, Ferreira TM, Costa AA (2021) Characterisation of the masonry building stock in Portugal for earthquake risk assessment. Eng Struct 233:111857. https://doi.org/10.1016/j.engstruct.2021.111857
Menichini G, Nistri V, Boschi S, Monte ED, Orlando M, Vignoli A (2022) Calibration of vulnerability and fragility curves from moderate intensity Italian earthquake damage data. Int J Disaster Risk Reduct 67:102676. https://doi.org/10.1016/j.ijdrr.2021.102676
Mulas MG, Stroffolini L, Martinelli P (2021) Vulnerability and retrofitting of torsionally deformable RC buildings: a case study. Structures 32:861–875. https://doi.org/10.1016/j.istruc.2021.03.063
Polese M, Marcolini M, Zuccaro G, Cacace F (2015) Mechanism based assessment of damage-dependent fragility curves for RC building classes. Bull Earthq Eng 13(5):1323–1345. https://doi.org/10.1007/s10518-014-9663-4
Qu Z, Dutu A, Zhong JR, Sun JJ (2015) Seismic damage of Masonry Infilled Timber Houses in the 2013 M7.0 Lushan Earthquake in China. Earthquake Spectra 31(3): 1859–1874. https://doi.org/10.1193/012914EQS023T
Ruggieri S, Tosto C, Rosati G, Uva G, Ferro A (2020) Seismic vulnerability analysis of masonry churches in piemonte after 2003 Valle Scrivia earthquake: post-event screening and situation 17 Years later. Int J Architect Heritage. https://doi.org/10.1080/15583058.2020.1841366
Ruggieri S, Cardellicchio A, Leggieri V, Uva G (2021) Machine-learning based vulnerability analysis of existing buildings. Autom Constr 132:103936. https://doi.org/10.1016/j.autcon.2021.103936
Saretta Y, Sbrogiò L, Valluzzi MR (2021) Seismic response of masonry buildings in historical centres struck by the 2016 Central Italy earthquake. Calibration of a vulnerability model for strengthened conditions. Construct Build Mater 299:123911. https://doi.org/10.1016/j.conbuildmat.2021.123911
Shin J, Choi I, Kim J (2021) Rapid decision-making tool of piloti-type RC building structure for seismic performance evaluation and retrofit strategy using multi-dimensional structural parameter surfaces. Soil Dyn Earthq Eng 151:106978. https://doi.org/10.1016/j.soildyn.2021.106978
Stocchi A, Giry C, Capdevielle S, Zentner I, Nayman E, Ragueneau F (2021) A simplified nonlinear modelling strategy to generate fragility curves for old masonry buildings. Comput Struct 254:106579. https://doi.org/10.1016/j.compstruc.2021.106579
Sun BT, Spencer BF, Yan PL, Chen X, Zhang GX (2021) Analysis of the seismic vulnerability of buildings in the Lushan Ms7.0 Earthquake in the Sichuan Province of China. J Earthquake Eng. https://doi.org/10.1080/13632469.2019.1692742
Zizi M, Corlito V, Lourenço PB, Matteis GD (2021) Seismic vulnerability of masonry churches in Abruzzi region, Italy. Structures 32:662–680. https://doi.org/10.1016/j.istruc.2021.03.013